

# Sulfidic Anion Concentrations on Early Earth for Surficial Origins-of-Life Chemistry

Sukrit Ranjan<sup>1,2,\*</sup>, Zoe R. Todd<sup>1</sup>, John D. Sutherland<sup>3</sup>, Dimitar D. Sasselov<sup>1</sup>

January 25, 2018

## ABSTRACT

A key challenge in origin-of-life studies is understanding the environmental conditions on early Earth under which abiogenesis occurred. While some constraints do exist (e.g., zircon evidence for surface liquid water), relatively few constraints exist on the abundances of trace chemical species, which are relevant to assessing the plausibility and guiding the development of postulated prebiotic chemical pathways which depend on these species. In this work, we combine literature photochemistry models with simple equilibrium chemistry calculations to place constraints on the plausible range of concentrations of sulfidic anions ( $\text{HS}^-$ ,  $\text{HSO}_3^-$ ,  $\text{SO}_3^{2-}$ ) available in surficial aquatic reservoirs on early Earth due to outgassing of  $\text{SO}_2$  and  $\text{H}_2\text{S}$  and their dissolution into small shallow surface water reservoirs like lakes. We find that this mechanism could have supplied prebiotically relevant levels of  $\text{SO}_2$ -derived anions, but not  $\text{H}_2\text{S}$ -derived anions. Radiative transfer modelling suggests UV light would have remained abundant on the planet surface for all but the largest volcanic explosions. We apply our results to the case study of the proposed prebiotic reaction network of Patel et al. (2015), and discuss the implications for improving its prebiotic plausibility. In general, epochs of moderately high volcanism could have been especially conducive to cyanosulfidic prebiotic chemistry. Our work can be similarly applied to assess and improve the prebiotic plausibility of other postulated surficial prebiotic chemistries that are sensitive to sulfidic anions, and our methods adapted to study other atmospherically-derived trace species.

*Subject headings:* Early Earth, Origin of Life, Prebiotic Chemistry, Volcanism, UV Radiation, Planetary Environments

---

<sup>1</sup>Harvard-Smithsonian Center for Astrophysics, Cambridge, MA 02138, USA

<sup>2</sup>MIT Dept. of Earth, Atmospheric, and Planetary Sciences, Cambridge, MA 02139, USA

<sup>3</sup>Medical Research Council Laboratory of Molecular Biology, Cambridge, CB2 0QH, UK

\*Corresponding author: 77 Massachusetts Avenue, Room 54-1719, Cambridge, MA 02139, USA; sukrit@mit.edu; t:617-253-6283, f:617-324-2055

## 1. Introduction

A key challenge for origins-of-life studies is determining the environmental conditions on early Earth. Environmental conditions (e.g., pH, temperature, pressure, chemical feedstock abundance, etc.) play a major role in determining the kinds of prebiotic chemistry that are possible or probable, and hence can help constrain the plausibility of proposed origin-of-life scenarios (e.g., Urey 1952, Corliss et al. 1981, McCollom 2013, Ruiz-Mirazo et al. 2014). Consequently, it is critical to understand the range of environmental conditions available on the early Earth for abiogenesis to proceed. Work over the past few decades has begun to constrain the environmental conditions that may have been available for abiogenesis, including but not limited to the past presence of liquid water, the availability of UV light at the surface, the mix of gases being outgassed to the atmosphere, the bulk pH of the ocean, and the conditions available at deep-sea hydrothermal vents (Bada et al. 1994; Farquhar et al. 2000; Mojzsis et al. 2001; Delano 2001; Holm and Charlou 2001; McCollom and Seewald 2007; Trail et al. 2011; Mulkidjanian et al. 2012; Beckstead et al. 2016; Sojo et al. 2016; Ranjan and Sasselov 2017; Novoselov et al. 2017; Halevy and Bachan 2017).

One challenging environmental factor to constrain is the abundance of trace chemical species on early Earth. These species can be important to proposed prebiotic chemical pathways as feedstocks or catalysts, but their abundances on the early Earth can be difficult to determine due to their rarity and hence limited impact on an already scarce rock record. In this paper, we explore the plausible abundances of one such family of molecules: sulfidic anions, i.e. sulfur-bearing aqueous anions (e.g., hydrosulfide,  $\text{HS}^-$ ; bisulfite,  $\text{HSO}_3^-$ ; sulfite,  $\text{SO}_3^{2-}$ ). Our initial interest in these molecules was stimulated by the role they play in the prebiotic chemistry proposed by Patel et al. (2015), but our calculations are applicable to studies of surficial prebiotic chemistry in general. For discussion of the relevance of the surface environment and its attendant processes to prebiotic chemistry, see, e.g., Mulkidjanian et al. (2012); Walker et al. (2012); Mutschler et al. (2015); Forsythe et al. (2015); Rapf and Vaida (2016); He et al. (2017); Deamer and Damer (2017). Our results are not relevant to deep-sea origin-of-life scenarios, such as McCollom and Seewald (2007); Larowe and Regnier (2008); Martin et al. (2008); Sojo et al. (2016).

We specifically explore the atmosphere as a planetary source for sulfidic anions through dissolution of volcanically outgassed  $\text{SO}_2$  and  $\text{H}_2\text{S}$  in small, shallow aqueous reservoirs like lakes. The prebiotic Earth’s atmosphere is thought to have been anoxic and more reducing than modern Earth (Kasting 2014), and volcanism levels have been hypothesized to have been higher (Richter 1985). Then the abundance of atmospheric  $\text{H}_2\text{S}$  and especially  $\text{SO}_2$  should have been higher compared to modern day levels, and aqueous reservoirs in equilibrium with the atmosphere would have dissolved some of these gases in accordance with Henry’s Law,

forming sulfidic anions through subsequent dissociation reactions. We use simple equilibrium chemistry combined with literature photochemical modelling to estimate the concentrations of these sulfidic anions as a function of  $p\text{SO}_2$  and  $p\text{H}_2\text{S}$ , and as a function of total sulfur outgassing flux. Elevated levels of atmospheric sulfur can lead to the formation of UV shielding gases and aerosols; consequently, we use radiative transfer calculations to constrain the surface UV radiation environment as a function of total sulfur outgassing flux. UV light is of interest to prebiotic chemists both as a potential stressor for abiogenesis (Sagan 1973; Cockell 2000), as a potential eustressor for abiogenesis (Sagan and Khare 1971; Mulkidjanian et al. 2003; Pascal 2012; Sarker et al. 2013; Rapf and Vaida 2016; Xu et al. 2016), and because of evidence that the nucleobases evolved in a UV-rich environment (Rios and Tor 2013; Beckstead et al. 2016).

We apply our calculations to the case study of the cyanosulfidic prebiotic systems chemistry of Patel et al. (2015). Building on the work of Powner et al. (2009) and Ritson and Sutherland (2012), Patel et al. (2015) proposed a prebiotic reaction network for the synthesis of activated ribonucleotides, short sugars, amino acids and lipid precursors from a limited set of feedstock molecules in aqueous solution under UV irradiation (at 254 nm). This reaction network is of interest because of the progress it makes towards the longstanding problem of nucleotide synthesis, because it offers the promise of a common origin for many biomolecules, and because it imposes specific geochemical requirements on its environment, which can be compared against what was available on early Earth to constrain and improve the chemistry’s prebiotic plausibility (Higgs and Lehman 2015; Springsteen 2015; Šponer et al. 2016). Relevant to our work, the Patel et al. (2015) chemistry requires sulfidic anions to proceed, as both a photoreductant and as a feedstock for a subset of the network’s reactions. Patel et al. (2015) proposed impactors as a source for the sulfidic anions; while possible, this scenario imposes an additional, local requirement for this chemistry to function. On the other hand, if the atmosphere could supply adequate sulfidic reductant (and feedstock) on a global basis, it would reduce the requirements for parts (or all) of this reaction network to function, and would make it more compelling as an origins-of-life scenario. We evaluate this scenario. While our paper focuses on the chemistry of Patel et al. (2015) as a case study, our work can be used to evaluate and improve the plausibility of any proposed sulfidic anion-sensitive surficial prebiotic chemistry. Our methods can be adapted to study the prebiotic surficial concentrations of other atmospherically-sourced aqueous species.

## 2. Background

### 2.1. Plausible Prebiotic Levels of H<sub>2</sub>S and SO<sub>2</sub>

The abundances of H<sub>2</sub>S and SO<sub>2</sub> in the Earth’s atmosphere are set by photochemistry, and are sensitive to a variety of factors. One of the most important of these factors is the outgassing rate of these compounds from volcanoes into the atmosphere. Absent biogenic sources, atmospheric photochemistry models typically assume abiotic SO<sub>2</sub> outgassing rates of  $1 - 3 \times 10^9 \text{ cm}^{-2} \text{ s}^{-1}$  (Kasting et al. 1989; Zahnle et al. 2006; Hu et al. 2013; Claire et al. 2014), consistent with the measured modern mean volcanogenic SO<sub>2</sub> outgassing rate of  $1.7 - 2.4 \times 10^9 \text{ cm}^{-2} \text{ s}^{-1}$  (Halmer et al. 2002). H<sub>2</sub>S emission rates are indirectly estimated and much less certain; they range from  $3.1 \times 10^8 - 7.7 \times 10^9 \text{ cm}^{-2} \text{ s}^{-1}$ . A common assumption in atmospheric modelling is that SO<sub>2</sub> and H<sub>2</sub>S are outgassed in a 10:1 ratio (e.g., Zahnle et al. 2006; Claire et al. 2014).

The early Earth is often hypothesized to have been characterized by higher levels of volcanic outgassing compared to the modern Earth due to presumed higher levels of internal heat and tectonic activity. Models often assume that Archaean SO<sub>2</sub> outgassing rates were  $\sim 3 \times$  modern (Richter 1985; Kasting et al. 1989; Zahnle et al. 2006). However, Halevy and Head (2014) point out that during the emplacement of major volcanogenic features such as the terrestrial basaltic plains, sulfur outgassing rates as high as  $10^{10} - 10^{11.5} \text{ cm}^{-2} \text{ s}^{-1}$  are possible, with the upper limit on outgassing rate coming from estimates of sulfur flux during emplacement of the Deccan Traps on Earth (Self et al. 2006).

No firm constraints exist for SO<sub>2</sub> and H<sub>2</sub>S levels on the prebiotic Earth. Kasting et al. (1989) modeled a plausible prebiotic atmosphere of 2 bars CO<sub>2</sub>, 0.8 bar N<sub>2</sub> atmosphere under  $0.75 \times$  present-day solar irradiation to account for the effects of the faint young Sun at 3.9 Ga. Kasting et al. (1989) assumed that sulfur was outgassed entirely as SO<sub>2</sub> at a total sulfur outgassing flux of  $\phi_S = 3 \times 10^9 \text{ cm}^{-2} \text{ s}^{-1}$  into an atmosphere overlying an ocean saturated in SO<sub>2</sub>; this last condition favors accumulation of SO<sub>2</sub> in the atmosphere. Claire et al. (2014) modeled an atmosphere of 0.99 bar N<sub>2</sub> and 0.01 bar CO<sub>2</sub>, under irradiation by the 2.5 Ga Sun, with an SO<sub>2</sub>:H<sub>2</sub>S outgassing ratio of 10:1, for  $\phi_S = 1 \times 10^8 - 1 \times 10^{10} \text{ cm}^{-2} \text{ s}^{-1}$ . Hu et al. (2013) modeled an atmosphere consisting of 0.9 bar CO<sub>2</sub> and 0.1 bar N<sub>2</sub> under irradiation by the modern Sun, with an SO<sub>2</sub>:H<sub>2</sub>S emission ratio of 2, for  $\phi_S = 3 \times 10^9 - 1 \times 10^{13} \text{ cm}^{-2} \text{ s}^{-1}$ . The SO<sub>2</sub> and H<sub>2</sub>S mixing ratios calculated by these models are shown in Table 1; these mixing ratios may be trivially converted to partial pressures by multiplying against the bulk atmospheric pressure. Note that the Claire et al. (2014) and Kasting et al. (1989) values are surface mixing ratios, while the Hu et al. (2013) values are column-integrated mixing ratios. Since H<sub>2</sub>S and SO<sub>2</sub> abundances tend to decrease with altitude due to losses from

photochemistry, column-integrated mixing ratios should be somewhat less than the surface mixing ratio. However, since density also decreases with altitude, mixing ratios at lower altitudes are more strongly weighted in the calculation of column-integrated mixing ratios, so the column-integrated mixing ratio tends to be close to the surface mixing ratio.

Table 1: Mixing ratios of H<sub>2</sub>S and SO<sub>2</sub> for different early Earth models in the literature and different  $\phi_S$ .

Model	$r_{H_2S}$	$r_{SO_2}$
Kasting et al. (1989) <sup>a</sup> , $\phi_S = 3 \times 10^9 \text{ cm}^{-2} \text{ s}^{-1}$	$2 \times 10^{-10}$	$2 \times 10^{-9}$
Claire et al. (2014) <sup>a</sup> , $\phi_S = 3 \times 10^9 \text{ cm}^{-2} \text{ s}^{-1}$	$1 \times 10^{-11}$	$5 \times 10^{-11}$
Hu et al. (2013) <sup>b</sup> , $\phi_S = 3 \times 10^9 \text{ cm}^{-2} \text{ s}^{-1}$	$4 \times 10^{-10}$	$3 \times 10^{-10}$
Claire et al. (2014) <sup>a</sup> , $\phi_S = 1 \times 10^{10} \text{ cm}^{-2} \text{ s}^{-1}$	$3 \times 10^{-11}$	$1 \times 10^{-10}$
Hu et al. (2013) <sup>b</sup> , $\phi_S = 1 \times 10^{10} \text{ cm}^{-2} \text{ s}^{-1}$	$1 \times 10^{-9}$	$9 \times 10^{-10}$

a: Surface mixing ratio

b: Column-integrated mixing ratio

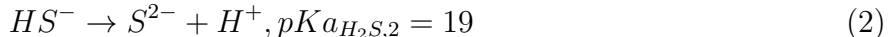
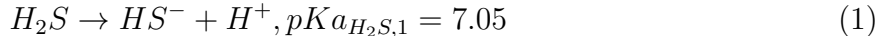
These models broadly agree that SO<sub>2</sub> and H<sub>2</sub>S levels were low and increase with sulfur emission rate, but their estimates for  $r_{SO_2}$  and  $r_{H_2S}$  disagree with each other by up to a factor of 400. The Hu et al. (2013) estimates are typically higher than the other estimates considered. The variation in these abundances demonstrates the sensitivity of SO<sub>2</sub> and H<sub>2</sub>S levels to atmospheric parameters such as composition and deposition velocities. Of these models, we find Hu et al. (2013) best matches the current fiducial understanding of conditions on early Earth: an atmosphere dominated by CO<sub>2</sub> and N<sub>2</sub>, with volcanic outgassing of both SO<sub>2</sub> and H<sub>2</sub>S, with oceans not saturated in SO<sub>2</sub> (as compared to possibilities for early Mars; see Halevy et al. 2007). Hu et al. (2013) also has the advantage of calculating atmospheric composition at higher values of sulfur outgassing flux than Kasting et al. (1989) and Claire et al. (2014), encompassing the  $1 \times 10^{11.5} \text{ cm}^{-2} \text{ s}^{-1}$  flux which is the upper limit of what Halevy and Head (2014) suggest possible for the emplacement of terrestrial basaltic plains. Hu et al. (2013) model processes including wet and dry deposition, formation of H<sub>2</sub>SO<sub>4</sub> and S<sub>8</sub> aerosol, and photochemistry and thermochemistry, with > 1000 reactions included in their reaction network. We therefore use Hu et al. (2013) as a guide when estimating H<sub>2</sub>S and SO<sub>2</sub> levels as a function of sulfur outgassing flux (see Appendix A), with the understanding that further, prebiotic-Earth specific modelling is required to constrain this relation with certainty.

### 3. Methods

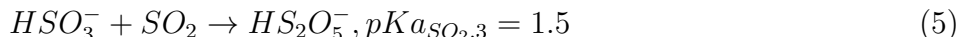
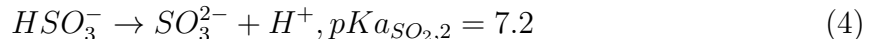
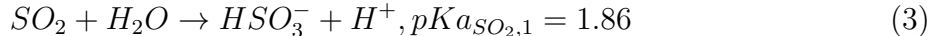
We consider a gas  $Z$  dissolving into a surficial aqueous reservoir ( $\lesssim 1$  m deep), through which the UV light required for prebiotic biomolecules synthesis can penetrate (Ranjan and Sasselov 2016); our archetypal such environment is a shallow lake. To isolate the effects of atmospheric supply of  $Z$ , we assume no other source of  $Z$  to be present (e.g., no geothermal source at the lake bottom). Henry’s Law states that the concentration of  $Z$ ,  $[Z]$ , in aqueous solution at the air/water interface is proportional to the partial pressure of the gas at that interface. We assume the aqueous reservoir to be well-mixed and equilibrated throughout, so that the concentration of  $[Z]$  is uniform throughout the reservoir at the surficial value. If the reservoir is not well-mixed, then the dissolved gas concentration will vary deeper into the reservoir. Under our assumption of no non-atmospheric source of  $Z$ ,  $[Z]$  would decrease with depth for a poorly-mixed aqueous reservoir.

This method of calculating  $[Z]$  is predicated on the assumption that the aqueous body is in equilibrium with the atmosphere, that is, that the solution is saturated in  $Z$  and the sink and source of  $Z$  is outgassing and deposition from the atmosphere. This assumption is valid when there are no other sinks to drive the system away from equilibrium. We discuss the veracity of this assumption in Section 5.2. In brief, this assumption is valid for shallow, well-mixed lakes that are not very acidic or hot, but not valid for deep, acidic, or hot waters. For these scenarios, our calculations provide upper bounds on  $[Z]$ .

In aqueous solution,  $H_2S$  undergoes the dissociation reactions



Where the  $pK_a$  values are taken from Lide (2009), and can be related to the corresponding equilibrium constants by  $K_{a_X} = 10^{-pK_{a_X}}$ . Similarly,  $SO_2$  undergoes the reactions



Where the  $pK_a$  values are from Neta and Huie (1985).

To compute the abundances of these different sulfur-bearing compounds as a function of  $[Z]$ , we must make assumptions as to the background chemistry of the aqueous reservoir they

are dissolved in, especially its pH. If the reservoir is completely unbuffered (e.g., pure water), its pH (and hence the speciation of S-bearing compounds) will be completely determined by  $[Z]$ . At the other extreme, if the reservoir is completely buffered, its pH will be independent of  $[Z]$ . Natural waters typically lie in between these two extremes; they are often buffered by mineral or atmospheric interactions towards a certain pH<sup>1</sup>, but with enough atmospheric supply their buffers can be overwhelmed. We explore these bracketing cases below, with the understanding that the true speciation behavior in nature was most likely somewhere in between.

### 3.1. Calculating Dissolved Gas Concentration

We use Henry’s law, coupled with the well-mixed reservoir assumption, to calculate the concentration of molecules dissolved from the atmosphere. Henry’s Law states that for a species  $Z$ ,

$$[Z] = H_Z f_Z, \tag{6}$$

where  $H_Z$  is the gas-specific Henry’s Law constant and  $f_Z$  is the fugacity of the gas. Over the range of temperatures and pressures relevant to surficial prebiotic chemistry, the gases in our study are ideal, and consequently  $f_Z = p_Z$ , the partial pressure of  $Z$ . We make this simplifying assumption throughout our study.

At  $T_0 = 298.15$  K, the Henry’s Law constants for  $H_2S$  and  $SO_2$  dissolving in pure water are  $H_{H_2S} = 0.101$  M/bar and  $H_{SO_2} = 1.34$  M/bar, respectively. Increasing salinity tends to decrease  $H_G$ , a process known as salting out. Similarly, increasing temperature also tends to decrease  $H_G$ . Our overall results are insensitive to variations in temperature of 25K from  $T_0$  and  $0 \leq [NaCl] \leq 1$  M; see Appendix C and Appendix D.1. For simplicity, we therefore neglect the temperature- and salinity-dependence of Henry’s Law.

---

<sup>1</sup>For example, the oceans on modern Earth are buffered to a pH of 8.1 – 8.2 due primarily to carbonate buffering (Hall-Spencer et al. 2008; Zeebe and Wolf-Gladrow 2009); estimates of ancient ocean pH vary, but often invoke slightly lower pH due to posited higher  $CO_2$  levels early in Earth’s history (see, e.g., Morse and Mackenzie 1998, Amend and McCollom 2009; Halevy and Bachan 2017 and sources therein). Smaller bodies, like lakes, can have an even wider range of pHs due to local conditions; lakes on modern Earth can have  $pH < 1$  (e.g., Kawah Ijen crater lake; Löhr et al. 2005), and  $pH > 11$  (e.g., Lake Natron; Grant and Jones 2000).

### 3.2. Unbuffered Solution

Consider an unbuffered solution with dissolved  $Z$ , whose properties are determined entirely by the reactions  $Z$  and its products undergo. From the definition of equilibrium constant, we can use the  $\text{H}_2\text{S}$  and  $\text{SO}_2$  speciation reactions to write:

$$\frac{a_{\text{HS}^-} a_{\text{H}^+}}{a_{\text{H}_2\text{S}}} = K a_{\text{H}_2\text{S},1} \quad (7)$$

$$\frac{a_{\text{S}^{2-}} a_{\text{H}^+}}{a_{\text{HS}^-}} = K a_{\text{H}_2\text{S},2} \quad (8)$$

and

$$\frac{a_{\text{HSO}_3^-} a_{\text{H}^+}}{a_{\text{SO}_2}} = K a_{\text{SO}_2,1} \quad (9)$$

$$\frac{a_{\text{SO}_3^{2-}} a_{\text{H}^+}}{a_{\text{HSO}_3^-}} = K a_{\text{SO}_2,2} \quad (10)$$

$$\frac{a_{\text{HS}_2\text{O}_5^-}}{a_{\text{SO}_2} a_{\text{HSO}_3^-}} = K a_{\text{SO}_2,3} \quad (11)$$

Where  $a_C$  is the activity of species  $C$ .  $a_C$  is related to the concentration of  $C$ ,  $[C]$ , by  $a_C = \gamma_C [C]$ , where  $\gamma_C$  is the activity coefficient (Misra 2012). The use of activities instead of concentrations accounts for ion-ion and ion- $\text{H}_2\text{O}$  interactions.  $\gamma = 1$  for a solution with an ionic strength of  $I = 0$ . For ionic strengths of 0-0.1 M, we calculate the activity coefficients for each species as a function of solution ionic strength using Extended Debye-Huckel theory (Debye and Huckel 1923). The activity coefficients in this formalism are calculated by:

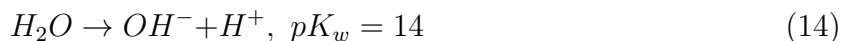
$$\log(\gamma_C) = -A z_C^2 \frac{I^{0.5}}{1 + B \alpha_C I^{0.5}} \quad (12)$$

Here,  $A$  and  $B$  are constants that depend on the temperature, density, and dielectric constant of the solvent; we use  $A = 0.5085 \text{ M}^{-1/2}$  and  $B = 0.3281 \text{ M}^{-1/2} \text{ \AA}^{-1}$ , corresponding to 25°C water (Misra 2012) (our results are robust to this assumption; see Appendix D).  $z_C$  is the charge of species  $C$ .  $\alpha_C$  is an ion-specific parameter with values related to the hydration radius of the aqueous species; we took our  $\alpha_C$  values from Misra (2012). We were unable to locate a value of  $\alpha_C$  for  $\text{HS}_2\text{O}_5^-$ , and consequently take  $\gamma_{\text{HS}_2\text{O}_5^-} = 1$  throughout.  $I$  is the ionic strength of the solution, defined as:



$$I = 0.5(\Sigma_C[C]z_C^2) \quad (13)$$

We can combine these equations with the equation for water dissociation:



$$(a_{H^+})(a_{OH^-}) = K_w \quad (15)$$

and the requirement for charge conservation:

$$\Sigma_C z_C [C] = 0 \quad (16)$$

With  $[Z]$  specified by Henry’s Law and our assumption of a well-mixed reservoir, this system is fully determined, and we can numerically solve it to determine the concentration of each of the species above as a function of  $pZ$  and  $I$ . A wide range of ionic strengths are possible for natural waters; modern freshwater systems like rivers have typical ionic strengths of order  $1 \times 10^{-3}M$  (Lerman et al. 1995), whereas modern terrestrial oceans have an ionic strength of  $0.7M$ <sup>2</sup>. The concentrations of divalent cations, especially  $Mg^{2+}$  and  $Ca^{2+}$ , in early oceans has been suggested to be near 10mM (Deamer and Dworkin 2005). A more fundamental constraint comes from vesicle formation, which is known to be inhibited at high salt concentrations and hence ionic strengths: Maurer and Nguyen (2016) report that lipid vesicle formation is impeded in solutions with  $I > 0.1M$ . These considerations motivate our focus on low ionic strength waters, with  $I \leq 0.1M$ <sup>3</sup>.

We calculate the speciation of sulfur-bearing species from dissolved  $H_2S$  and  $SO_2$  for  $I = 0$  and  $I = 0.1M$ ; the results are shown in Figs. 1 and 2.  $I = 0$  is the lowest possible ionic strength, and  $I = 0.1M$  corresponds to the limit from lipid vesicle formation.

### 3.3. Buffered Solution

Consider now an aqueous reservoir that is buffered to a given pH. For example, the pH of the modern oceans is buffered by calcium carbonate to a global mean value of 8.1 – 8.2

---

<sup>2</sup><http://www.aqion.de/site/69>, accessed 29 November 2016

<sup>3</sup>A further practical challenge with extending our calculations to higher ionic strengths is that the parameters required to compute the activity coefficients at high ionic strengths (e.g., via the Truesdell and Jones 1974 formalism) are not available for many of the species we consider.

(Hall-Spencer et al. 2008). Then, we know  $[H^+]$ , and can hence calculate the speciation of dissolved  $H_2S$  and  $SO_2$  from the equilibrium constant equations 7-8 and 9-11 individually. Our results are insensitive to ionic strength for  $I \leq 0.1M$  (see Figs. 1 and 2, and Appendix B), and  $I \leq 0.1M$  is required for vesicle formation and other prebiotic chemistry (Maurer and Nguyen 2016; Deamer and Damer 2017), motivating us to take  $I = 0$  for simplicity.

With Henry’s Law and our assumption of a well-mixed reservoir, we can readily calculate the concentration of the above species as a function of  $pH_2S$  or  $pSO_2$  and  $pH$ . The results of this calculation are presented in Figs. 1 and 2 for three representative  $pH$ s. We selected  $pH=8.2$ , corresponding to modern ocean;  $pH=7$ , corresponding to the near-neutral phosphate-buffered conditions in which Patel et al. (2015) conducted their experiments; and  $pH=4.25$ , corresponding to raindrops in a  $pCO_2 \sim 0.1$  bar atmosphere (Halevy et al. 2007). Such high  $CO_2$  levels are hypothesized for the young Earth in order to power a greenhouse effect large enough to maintain clement surface conditions (Kasting 1993).

The code used to implement these calculations is available for validation and extension at <https://github.com/sukritranjan/RanjanToddSutherlandSasselov2017.git>.

## 4. Results

### 4.1. $H_2S$ vs $SO_2$

Fig. 1 shows the speciation of sulfur-bearing compounds from dissolved  $H_2S$  for an unbuffered reservoir, and reservoirs buffered to various  $pH$ s. Over the range of ionic strengths considered,  $HS^-$  is the dominant anion, and  $S^{2-}$  is present at negligible concentrations. As  $pH_2S$  increases, the  $pH$  of the unbuffered reservoir drops, but slowly. This is expected, since  $H_2S$  is a weak acid.

Fig. 2 shows the speciation of sulfur-bearing compounds from dissolved  $SO_2$  for an unbuffered reservoir, and reservoirs buffered to various  $pH$ s. Because of the lack of  $O_2$  in this anoxic era, the first dissociation of  $SO_2$  forms sulfite, rather than sulfate.  $HSO_3^-$  and  $SO_3^{2-}$  are present at comparable levels;  $HS_2O_5^-$  is negligible. As  $pSO_2$  increases, the  $pH$  of the unbuffered reservoir falls off rapidly; this is expected since hydrated  $SO_2$  is a strong acid.

$SO_2$  is an order of magnitude more soluble than  $H_2S$ , and its first dissociation is much more strongly favored ( $pKa_{SO_2,1} = 1.86$  vs  $pKa_{H_2S,1} = 7.05$ ). Consequently, far higher concentrations of sulfidic anions can be sustained for a given  $pSO_2$  than for the same  $pH_2S$  (see Figs. 1 and 2). Maintaining micromolar concentrations of  $HS^-$  requires  $pH_2S \geq 1 \times 10^{-6}$  bar at  $pH=8.2$  (modern ocean), and  $pH_2S \geq 1 \times 10^{-5}$  bar for more neutral  $pH$ s. Maintain-

ing micromolar concentrations of  $S^{2-}$  is impossible over plausible ranges of pH and sulfur outgassing flux ( $pK_{a_{H_2S,2}} = 19$ ). The concentration of sulfidic anions could be increased by going to higher pH and salinity. However, the reactions of, e.g., Patel et al. (2015) have not been demonstrated to proceed under such conditions.

By contrast, dissolved  $SO_2$  gives rise to comparatively high concentrations of sulfidic anions due to higher solubility and a more favorable first ionization. Micromolar concentrations of  $HSO_3^-$  are possible for  $pSO_2 > 1 \times 10^{-11}$  bar for all but very acidic solutions; micromolar concentrations of  $SO_3^{2-}$  are possible for solutions buffered to  $pH \geq 7$  over the same range. *Millimolar* levels of  $HSO_3^-$  and  $SO_3^{2-}$  are possible for solutions buffered to  $pH \geq 8.2$  for  $pSO_2 \gtrsim 10^{-10}$  bar, and for  $pH \geq 7$  solutions for  $pSO_2 \gtrsim 10^{-8}$  bar.  $pSO_2 \geq 3 \times 10^{-10}$  bar is expected for outgassing rates corresponding to the steady-state on early Earth according to the model of Hu et al. (2013) ( $\phi_S = 3 \times 10^9 \text{ cm}^{-2} \text{ s}^{-1}$ ). During transient epochs of intense volcanism such as the emplacement of basaltic plains, emission rates might have risen as high as  $\phi_S = 10^{11.5} \text{ cm}^{-2} \text{ s}^{-1}$  (Halevy and Head 2014; Self et al. 2006), corresponding to  $pSO_2 = 1 \times 10^{-8}$  bar. We note that estimates based on Hu et al. (2013) are for column-integrated abundances, and the surface abundances were likely modestly larger. Hence, it seems likely that the atmosphere could have supplied micromolar-levels of  $SO_2$ -derived anions for prebiotic chemistry, and perhaps even millimolar concentrations if the solution were buffered to slightly alkaline pH (e.g., pH comparable to the modern ocean).

## 4.2. $H_2S$ and $SO_2$

In Section 4.1 we evaluated the prospects for buildup of sulfur-bearing anions from dissolved atmospheric  $H_2S$  and  $SO_2$  in isolation. However,  $H_2S$  and  $SO_2$  are injected simultaneously into the atmosphere by volcanism, and would have been present at the same time. Fig. 3 presents the speciation of sulfur-bearing molecules from dissolved atmospheric  $H_2S$  and  $SO_2$  in a solution buffered to  $pH = 7$  as a function of total sulfur outgassing rate,  $\phi_S$ . This pH corresponds approximately to the phosphate-buffered conditions in which the chemistry of Patel et al. (2015) proceeded<sup>4</sup>. If the solution were buffered to higher pH sulfidic anion concentrations would be higher due to a more favorable first dissociation, and vice versa.

As before, we connected the  $H_2S$  and  $SO_2$  abundances connected to  $\phi_S$  by the high- $CO_2$  model calculations of Hu et al. (2013). We took the surface mixing ratio of these

---

<sup>4</sup>It is thought that these chemistries should proceed over a broad range of pH. However, they will proceed best for  $pH \lesssim 9.2$  (so that HCN tends to remain protonated) and  $pH \gtrsim 7$  (so that the sulfidic anions tend to remain deprotonated)

gases to equal the column-integrated mixing ratio, which may slightly underestimate the surface mixing ratio of these gases.  $\phi_S = 1 - 3 \times 10^9 \text{ cm}^{-2} \text{ s}^{-1}$  for modern Earth, and  $\phi_S = 10^{10} - 10^{11.5} \text{ cm}^{-2} \text{ s}^{-1}$  have been suggested on a transient (1-10 year) basis for major volcanic episodes like the emplacement of basaltic plains on Earth (Halevy and Head 2014; Self et al. 2006). As discussed in Section 4.1,  $\text{SO}_2$ -derived anions can build to micromolar levels at modern outgassing rates, and can build to millimolar levels during volcanic episodes like the emplacement of basaltic plains, while  $\text{H}_2\text{S}$ -derived anions cannot, absent highly alkaline conditions.

### 4.3. Coupling to the UV Surface Environment

$\text{H}_2\text{S}$ ,  $\text{SO}_2$ , and their photochemical aerosol by-products ( $\text{S}_8$ ,  $\text{H}_2\text{SO}_4$ ) are robust UV shields, and at elevated levels their presence can dramatically reduce surface UV radiation (Hu et al. 2013; Ranjan and Sasselov 2017). This effect could be good for origin-of-life scenarios which do not require UV light, since UV light can photolytically destroy newly formed biomolecules (e.g., Sagan 1973). On the other hand, it could be bad for UV-dependent prebiotic chemistry, which depend on UV light to power their syntheses (e.g., Ritson and Sutherland 2012, Patel et al. 2015, Xu et al. 2016). In the latter case, it begs the question whether the elevated levels of  $\text{SO}_2$  and  $\text{H}_2\text{S}$  that could supply the sulfidic anions required for cyanosulfidic chemistry might also quench the UV radiation also required by these pathways.

To explore this question, we calculated the attenuation of incoming 3.9 Ga solar radiation (calculated from the models of Claire et al. 2012) by an  $\text{CO}_2$ - $\text{N}_2$ - $\text{SO}_2$ - $\text{H}_2\text{S}$  atmosphere, using a two-stream radiative transfer model (Ranjan and Sasselov 2017; Ranjan et al. 2017). We set the solar zenith angle to  $48.2^\circ$ , corresponding to the insolation-weighted mean value (Cronin 2014), and the albedo to 0.2, a representative value for rocky planets consistent with past modelling<sup>5</sup> (Segura et al. 2003; Rugheimer et al. 2015). We once again used the work of Hu et al. (2013) to connect  $\text{H}_2\text{S}$  and  $\text{SO}_2$  abundances to  $\phi_S$ , and for consistency we assumed inventories of  $\text{CO}_2$  and  $\text{N}_2$  matching those assumed by Hu et al. (2013) (their high- $\text{CO}_2$  case). Our radiative transfer calculations are insensitive to the atmospheric T/P profile, because atmospheric emission is negligible at UV wavelengths and our UV cross-sections vary minimally as a function of temperature (Ranjan et al. 2017); consequently, we assume a simple exponential profile to the vertical number density of the atmosphere. We also used the work of Hu et al. (2013) to estimate the total  $\text{S}_8$  and  $\text{H}_2\text{SO}_4$  aerosol loading in the atmosphere for each  $\phi_S$ , and calculated aerosol optical parameters using the same size

---

<sup>5</sup>Our results are insensitive to the precise choice of albedo or solar zenith angle

distributions and complex indices of refraction as they did. Lacking detailed atmospheric profiles of the aerosol abundance as a function of altitude, we assumed the aerosols were distributed exponentially, with a scale height equal to the bulk atmosphere scale height (i.e. well-mixed). In practice, sulfur aerosols tend to form photolytically at higher altitudes, meaning our approach places more aerosol at low altitude and less aerosol at high altitude. Since the radiative impact of aerosol absorption is amplified lower in the atmosphere due to enhanced scattering, this means our treatment should slightly overestimate UV attenuation due to aerosols. Similarly, Hu et al. (2013) assume an aerosol size distribution with surface area mean diameter  $D_S = 0.1\mu m$ , at the lower end of the plausible  $D_S = 0.1 - 1\mu m$  range, which maximizes the possible radiative impact of the sulfur aerosols. Consequently, our results should be interpreted as a lower bound on the true UV fluence.

Fig. 4 presents the UV fluence available on the surface of the prebiotic Earth as a function of  $\phi_S$  under these assumptions. For  $\phi_S \leq 1 \times 10^{11} \text{ cm}^{-2} \text{ s}^{-1}$ , UV radiation remains abundant on the planet surface. Millimolar levels of  $\text{SO}_3^{2-}$  and  $\text{HSO}_3^-$  are available in aqueous reservoirs buffered to  $pH \geq 7$  for  $\phi_S = 1 \times 10^{11} \text{ cm}^{-2} \text{ s}^{-1}$ . Consequently, volcanism could supply prebiotically relevant levels of  $\text{SO}_3^{2-}$  and  $\text{HSO}_3^-$  without blocking off the UV radiation required by UV-dependent prebiotic pathways for sulfur emission fluxes up to  $\phi_S \leq 1 \times 10^{11} \text{ cm}^{-2} \text{ s}^{-1}$  (near the upper edge of what is considered plausible for major terrestrial volcanic episodes). On the other hand, for  $\phi_S \geq 3 \times 10^{11} \text{ cm}^{-2} \text{ s}^{-1}$ , atmospheric sulfur-bearing gases and aerosols, especially the UV-absorbing  $\text{S}_8$ , suppress surface UV radiation by an order of magnitude or more; this paucity of UV radiation may pose a challenge for UV-dependent prebiotic chemistry, but could create a very clement surface environment for UV-independent prebiotic chemistries. If one accepts the idea that the nucleobases show evidence of UV selection pressure (Crespo-Hernández et al. 2004; Serrano-Andres and Merchan 2009; Rios and Tor 2013; Beckstead et al. 2016; Pollum et al. 2016), this suggests the biogenic nucleobases evolved in an epoch with  $\phi_S \leq 1 \times 10^{11} \text{ cm}^{-2} \text{ s}^{-1}$ .

## 5. Discussion

### 5.1. Sulfidic Anion Concentrations in Surficial Waters on Early Earth

We have shown that terrestrial volcanism could have globally supplied the sulfidic anions  $\text{SO}_3^{2-}$  and  $\text{HSO}_3^-$ , derived from the dissolution of  $\text{SO}_2$  into aqueous solution, to shallow surficial aqueous reservoirs on early Earth. These compounds would have been available at micromolar levels for volcanic outgassing rates comparable to the modern day. During episodes of high volcanism, such as those responsible for emplacement of basaltic plains ( $\phi_S \approx 1 \times 10^{11} \text{ cm}^{-2} \text{ s}^{-1}$ ), these compounds could have built up to the millimolar levels in

shallow aqueous reservoirs buffered to  $\text{pH} \geq 7$ . On the other hand, due to its lower solubility and unfavorable first dissociation, sulfidic anions derived from dissolving atmospheric  $\text{H}_2\text{S}$  can only be supplied at low concentrations (sub-micromolar) across the plausible range of  $\text{pH}_2\text{S}$  and  $\text{pH}$ <sup>6</sup>. Therefore, other mechanisms must be invoked for supply of such anions, if required by a proposed prebiotic chemical pathway.

We conducted our calculations assuming a temperature of  $T = 25^\circ\text{C}$ . We investigate the sensitivity of our results to temperatures ranging from  $T = 0\text{--}50^\circ\text{C}$  in Appendix D, including temperature effects on both the reaction rate and the Henry’s Law coefficient. While  $\text{H}_2\text{S}$ -derived anion concentrations are not significantly affected by temperature variations in this range,  $\text{SO}_2$ -derived anion concentrations are. This is because  $H_{\text{SO}_2}$  decreases with temperature and  $\text{pK}_{\text{a}_{\text{SO}_2,1}}$  increases with temperature<sup>7</sup>; both effects favor increased concentrations of  $\text{HSO}_3^-$  and its derivatives, assuming a not-highly acidic ( $\text{pH} > 2.5$ ) solution. We find that while our overall conclusions are unchanged, concentrations of the  $\text{SO}_2$ -derived anions  $\text{HSO}_3^-$  and  $\text{SO}_3^{2-}$  are an order of magnitude higher for  $T \approx 0^\circ\text{C}$  relative to  $T = 25^\circ\text{C}$ , and an order of magnitude lower for  $T \approx 50^\circ\text{C}$ , assuming a near-neutral reservoir. Consequently, cooler waters are more favorable environments for prebiotic chemistry which invokes  $\text{HSO}_3^-$  or  $\text{SO}_3^{2-}$ .

Sulfur-bearing gases and aerosols, in particular  $\text{S}_8$ , are strong UV absorbers, and if present at high enough levels could suppress UV-sensitive prebiotic chemistry. For  $\phi_S \leq 1 \times 10^{11} \text{ cm}^{-2} \text{ s}^{-1}$ , corresponding to most of the plausible range of sulfur emission fluxes on early Earth, surface UV fluxes (200-300 nm) are not significantly attenuated by atmospheric absorbers, meaning that in the steady state and for most volcanic eruptions, abundant UV light should have reached the Earth’s surface to power UV-dependent prebiotic chemistry. However, for the very largest volcanic eruptions, corresponding to the uppermost end of the plausible range of sulfur outgassing fluxes during terrestrial basaltic flood plain emplacement ( $\phi_S = 3 \times 10^{11} \text{ cm}^{-2} \text{ s}^{-1}$ ), surface UV fluence (200-300 nm) may be reduced by an order of magnitude or more. Hence, the very largest volcanic events<sup>8</sup> might create an especially

---

<sup>6</sup>Our results are relevant to shallow, aqueous bodies of water, like lakes. By contrast, in the ocean volcanoes vent directly into the water, and the turnover time can be long. Consequently, one could envision significant buildup of  $\text{H}_2\text{S}$  near deep-ocean volcanoes. This scenario is beyond the scope of this work, but may be worthy of consideration for  $\text{HS}^-$ -dependent chemistry

<sup>7</sup>The exothermic first dissociation of  $\text{SO}_2$  is disfavored at higher temperatures.

<sup>8</sup>However, even in this case there may be a window in which prebiotic chemistry experiences both elevated  $\text{SO}_2$  levels and plenty of UV light, since aerosol formation is not instantaneous. Detailed photochemical modelling is required to determine the timescale of aerosol formation after a large volcanic eruption on early Earth; absent such modelling, we note that on modern Earth, formation of sulfate aerosols from volcanic

clement surficial environment for UV-independent prebiotic chemistry

These results were derived using the high-CO<sub>2</sub> model of Hu et al. (2013), which, while plausible, assumes more CO<sub>2</sub> and less N<sub>2</sub> than other models of prebiotic Earth (e.g., Rugheimer et al. 2015), and is hence comparatively oxidizing. We explored the sensitivity of our results to this assumption via the the N<sub>2</sub>-rich model of Hu et al. (2013). This model assumes 1 bar of N<sub>2</sub> and negligible CO<sub>2</sub>, and is hence an unrealistic approximation to the early Earth, because an appreciable CO<sub>2</sub> inventory is expected due to climate constraints (Kasting 1993; Wordsworth and Pierrehumbert 2013), and due to volcanic outgassing of CO<sub>2</sub>. Hence, this model serves as an extreme bounding case. Assuming this model, we find that H<sub>2</sub>S and SO<sub>2</sub> levels are lower than for the high-CO<sub>2</sub> case. SO<sub>2</sub>-derived anions remain available at micromolar levels over the plausible range of  $\phi_S$ , but in order to build to millimolar levels require the assumption of reservoirs buffered to slightly alkaline pH (e.g., pH $\sim$  8.2, modern ocean). HS<sup>-</sup> levels are even lower than in the CO<sub>2</sub>-rich case. UV fluences are lower than in the CO<sub>2</sub>-rich case, due to elevated levels of S<sub>8</sub> formation in this more reducing atmosphere; surface UV fluence (200-300 nm) is suppressed by an order of magnitude or more for  $\phi_S \geq 1 \times 10^{11} \text{ cm}^{-2} \text{ s}^{-1}$ . Overall, this boundary case suggests that our finding that the atmosphere can supply prebiotically-relevant levels of SO<sub>2</sub>-derived anions but not H<sub>2</sub>S-derived anions in conjunction with UV light remains true across a broad range of CO<sub>2</sub> and N<sub>2</sub> abundances, though both sulfidic anion abundances and UV are lower for more reducing, N<sub>2</sub>-rich atmospheres. However a detailed exploration of the pCO<sub>2</sub>-pN<sub>2</sub> parameter space with photochemical models is required to be certain of these findings.

## 5.2. Impact of Other Sinks

Our analysis is predicated on the assumption that [Z] is set by Henry equilibrium, i.e. that the aqueous reservoir is saturated in H<sub>2</sub>S and SO<sub>2</sub>. This assumes no major sinks other than outgassing to the atmosphere. In this section, we examine the sensitivity of our results to this assumption. Microbial sinks (e.g., Halevy 2013) are not relevant since we are concerned with prebiotic Earth; neither are oxic sinks, since the surface of early Earth was anoxic (Kasting and Walker 1981; Kasting 1987; Farquhar et al. 2001; Pavlov and Kasting 2002; Li et al. 2013). However, reactions with metal cations to produce insoluble precipitates and redox reactions could have been relevant; we explore these sinks.

---

eruptions occurs on a timescale of weeks (Robock 2000); we may speculate a similar timescale for aerosol formation on early Earth.

### 5.2.1. Precipitation Reactions with Metal Cations

We explored the possibility that reactions of S-anions with metal cations might lead to formation of insoluble precipitates, which would act as a sink on S-anion concentrations. Such cations might have been delivered to aqueous reservoirs via weathering of rocks and minerals.

Under standard conditions,  $\text{Fe}^{2+}$  and  $\text{Cu}^{2+}$  react with  $\text{H}_2\text{S}(\text{aq})$  to generate insoluble precipitates, like  $\text{CuS}$  and  $\text{FeS}_2$  (Rumble 2017; Rickard and Luther 2007). Interaction of copper sulfides with cyanide solution can liberate  $\text{HS}^-$  (Coderre and Dixon 1999), as invoked by Patel et al. (2015). In general high-Cu/Fe waters (e.g. due to interaction with ores) will be even more  $\text{HS}^-$ -poor than we have modeled, with the caveat that specific local environmental factors (like the presence of aqueous cyanide) can prevent sulfide depletion due to precipitation. This reinforces our conclusion that  $\text{HS}^-$  concentrations are unlikely to have reached prebiotically relevant levels on early Earth, absent unique local factors. For example, the aqueous cyanide required as a feedstock in the pathways of Patel et al. (2015) would also permit elevated  $\text{HS}^-$  levels.

$\text{Ca}^{2+}$ , produced by mineral weathering, reacts with sulfite to produce insoluble  $\text{CaSO}_3$ . Studying the  $\text{Ca}^{2+}$ - $\text{SO}_3^{2-}$  system requires considering the effects of carbonate ( $\text{CO}_3^{2-}$ ) as well, because  $\text{Ca}^{2+}$  forms precipitate with this anion as well, and because high levels of carbonate are expected in natural waters on early Earth due to elevated levels of atmospheric  $\text{CO}_2$  required to solve the faint young Sun paradox (Kasting 1987). While precisely modeling this geochemical system requires use of a geochemical model capable of accounting for all reactions involving sulfites and carbonates and their kinetics, we can get a first-order estimate of the impact of  $\text{Ca}^{2+}$ , as follows. Assuming parameters from Hu et al. (2013), the flux of carbonates into solution due to deposition and speciation of atmospheric  $\text{CO}_2$  is  $r_{\text{CO}_2} n_{\text{atm}} v_{\text{dep,CO}_2} = 2 \times 10^{15} \text{ cm}^{-2} \text{ s}^{-1}$  on the  $\text{CO}_2$ -rich early Earth, which exceeds the mean flux of Ca due to mineral weathering ( $1 - 5 \times 10^{10} \text{ cm}^{-2} \text{ s}^{-1}$ ; Taylor et al. 2012; Watmough and Aherne 2008) by 5 orders of magnitude; thus, it is reasonable to assume the solution is saturated in  $\text{CO}_2$  with abundance dictated by Henry’s law of  $(3.3 \times 10^{-2} \text{ M}/\text{bar})(0.9 \text{ bar}) = 0.03\text{M}$  (Sander 2015). Then,  $[\text{CO}_3^{2-}] = (0.03\text{M})(10^{7-6.35})(10^{7-10.33}) = 6 \times 10^{-5}\text{M}$  at neutral pH (dissociation constants  $K_{a_{\text{CO}_2,1}} = 6.35$  and  $K_{a_{\text{CO}_2,2}} = 10.33$  from Rumble (2017)<sup>9</sup>). Since  $\text{CaCO}_3$  ( $K_{sp} = 3.36 \times 10^{-9} \text{ M}^2$ , Rumble 2017) is two orders of magnitude less soluble than  $\text{CaSO}_3$  ( $K_{sp} = 3.1 \times 10^{-7} \text{ M}^2$ , Rumble 2017) and the sulfite flux is much less than the

---

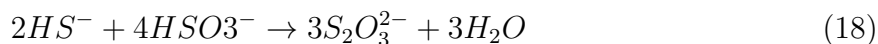
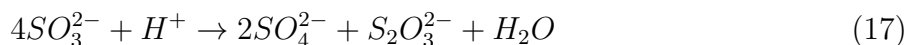
<sup>9</sup>Using pKas for  $\text{CO}_2$  dissociation from modern seawater, e.g., Zeebe and Wolf-Gladrow (2009), results in much higher carbonate levels, much lower Ca levels, and a much higher threshold for  $\text{CaSO}_3$  saturation, so this treatment is conservative.



carbonate flux, we can assume that  $[\text{Ca}^{2+}]$  is dictated to first order by equilibrium with carbonate mineral, i.e.  $[\text{Ca}^{2+}] = 3.36 \times 10^{-9} \text{M}^2 / 6 \times 10^{-5} \text{M} = 6 \times 10^{-5} \text{M}$ . At this  $[\text{Ca}^{2+}]$ ,  $\text{CaSO}_3^{2-}$  (s) will begin to form at  $[\text{SO}_3^{2-}] = 3.1 \times 10^{-7} \text{M}^2 / 6 \times 10^{-5} \text{M} = 5 \times 10^{-3} \text{M}$ . The  $[\text{SO}_3^{2-}]$  we calculate does not exceed this threshold value across the plausible range of sulfur outgassing fluxes in our calculation, meaning the solution is unsaturated in  $\text{CaSO}_3$  and precipitate does not form. Were  $p\text{CO}_2$  lower, e.g.,  $p\text{CO}_2 = 0.2 \text{ bar}^{10}$ ,  $\text{CaSO}_3$  precipitate formation begins at  $[\text{SO}_3^{2-}] = 1 \times 10^{-3} \text{M}$ . However, if pH were low, the carbonate solubility would exceed sulfite solubility, and sulfite precipitates would form (Halevy et al. 2007); hence at low pH, sulfite and bisulfite concentrations will be below the values we calculate. Overall, our results are unaffected by  $\text{CaSO}_3$  precipitation across most of parameter space, but  $\text{CaSO}_3$  precipitation might be a significant sink on aqueous sulfite levels for acid solutions and/or for very low atmospheric  $\text{CO}_2$ -levels; calculations with a more thorough geochemical model (e.g., PHREEQC, Parkhurst and Appelo 2013) are required to constrain S-anion concentrations in this regime.

### 5.2.2. Redox Reactions

We explored the possibility that redox reactions (disproportionation, comproportionation) might have acted as sinks to S-anion concentrations in shallow aqueous reservoirs on prebiotic Earth, or might otherwise affect the distribution of sulfidic anions. We identified the following reactions that are spontaneous near standard conditions (Siu and Jia 1999; Halevy 2013):



The kinetics of Reaction 17 are not well characterized near standard temperature, and are an active topic of research (Mirzoyan and Halevy 2014; Amshoff et al. 2016). Meyer et al. (1982) report sulfite and bisulfite are stable on timescales  $\geq 1$  year in anoxic conditions, while Guekezian et al. (1997) report decay of sulfite in days at  $\text{pH} \geq 12.8$ . Halevy (2013) propose that rate coefficients in the range  $k_{17} = \exp(\frac{-50\text{kJmol}^{-1}}{RT}) - \exp(\frac{-40\text{kJmol}^{-1}}{RT}) \text{ s}^{-1}$  are plausible; at 293K, this corresponds to  $1 \times 10^{-9} - 7 \times 10^{-8} \text{ s}^{-1}$ , which correspond to timescales of 0.5–30 years. The kinetics of Reaction 18 have been determined as a function of temperature at

---

<sup>10</sup>Corresponding to the lower limit suggested by Kasting (1987) from climate considerations.

pH=9 and  $I = 0.2\text{M}$  by Siu and Jia (1999). At 293K, the rate coefficient is  $k_{18} = 4 \times 10^3 \text{ M}^{-2} \text{ s}^{-1}$ . At the S-anion concentrations relevant to our work<sup>11</sup>, the timescale of this reaction is  $\gtrsim 1$  year. For comparison, putative prebiotic chemistry in laboratory studies often occurs on timescales of hours to days (Patel et al. 2015; Xu et al. 2017, e.g., ).

We test the effects of redox reactions on S-anion concentrations by carrying out a dynamical equilibrium calculation for a shallow lake buffered to pH=7, with source the atmosphere and sink these redox reactions. Following the treatment of Halevy (2013), the equilibrium equations can be written:

$$r_{H_2S} n_{atm} v_{dep, H_2S} A_{catch} = \left(\frac{2}{3} k_{18} [HS^-][HSO_3^-]^2\right) A_{lake} d_{lake} \quad (19)$$

$$r_{SO_2} n_{atm} v_{dep, SO_2} A_{catch} = \left(\frac{4}{3} k_{18} [HS^-][HSO_3^-]^2 + k_{17} [S(IV)]\right) A_{lake} d_{lake} \quad (20)$$

For consistency with Hu et al. (2013), we adopt  $v_{dep, H_2S} = 0.015 \text{ cm s}^{-1}$ ,  $v_{dep, SO_2} = 1 \text{ cm s}^{-1}$ ,  $T = 288\text{K}$ , and  $n_{atm} = \frac{1\text{bar}}{kT} = 2.4 \times 10^{19} \text{ cm}^{-3}$ . Since we are concerned with shallow, well-mixed lakes, we take the lake depth  $d_{lake} = 10^2 \text{ cm}$ .  $A_{catch}$  is the catchment area of the lake and  $A_{lake}$  is the surface area of the lake; we conservatively adopt  $A_{catch} = A_{lake}$ , which likely underestimates sulfur supply since the catchment area is often larger than the lake area.  $[S(IV)]$  refers to the total concentration of S(IV) atoms in solution, and is calculated as  $[S(IV)] = [SO_2] + [HSO_3^-] + [SO_3^{2-}] + 2[HS_2O_5^-] \approx [SO_2(aq)] + [HSO_3^-] + [SO_3^{2-}]$ <sup>12</sup>. Since we have specified pH=7 and know the relevant pKas, we can calculate  $[HSO_3^-]$  from  $[S(IV)]$  and vice versa. With  $r_{H_2S}$  and  $r_{SO_2}$  specified from Hu et al. (2013), we have a system of two equations in two variables that we can solve. Figure 5 shows the resultant S-anion concentrations as a function of  $\phi_S$ .

The dynamic calculation is very sensitive to the uncertainty in  $k_{17}$ , with sulfite and bisulfite concentrations varying by 2 orders of magnitude and hydrosulfide concentrations varying by 4 across the range of  $k_{17}$  suggested by Halevy (2013). However, even with this uncertainty it is clear that prebiotically relevant levels ( $\geq 1\mu\text{M}$ ) of  $SO_2$ -derived anions are available across the range of plausible sulfur outgassing fluxes, with concentrations  $\sim 1 - 10\mu\text{M}$  if sulfite disproportionation is fast and  $\sim 100 - 1000\mu\text{M}$  if sulfite disproportionation is slow. Note depending on  $k_{17}$ , it is possible for  $[HS^-]$  in the dynamic calculation to exceed the value calculated from solubility constraints; in reality, in well-mixed solution  $H_2S$  would de-gas when it reached the solubility limit, voiding equation 19. In these cases,  $[HS^-]$  is lower than the value calculated from the dynamic method, modestly increasing sulfite and bisulfite

---

<sup>11</sup> $[HS^-] \lesssim 10^{-8}\text{M}$ ,  $[HSO_3^-] \lesssim 10^{-3}\text{M}$

<sup>12</sup> $[HS_2O_5^-]$  is negligible for dilute  $[SO_2]$

concentrations since Reaction 18 is slower. S-anion concentrations increase as  $d_{lake}$  and  $T$  decrease, and are ultimately limited by gas solubility. Overall, our finding that prebiotically relevant levels of  $\text{SO}_2$ -derived anions were available in shallow well-mixed lakes on early Earth is robust to the effect of redox reactions, but it is possible for the precise concentrations to be lower than from our equilibrium calculation depending on the depth and temperature of the lake, and especially on the rate of sulfite disproportionation  $k_{17}$ . Constraining  $k_{17}$  is key to improved modelling of abiotic sulfur chemistry.

### 5.3. Case Study: Implications for Cyanosulfidic Systems Chemistry of Patel et al. (2015)

The cyanosulfidic prebiotic chemistry of Patel et al. (2015) requires cyanide and sulfur-bearing anions, both as feedstocks and as sources of hydrated electrons through UV-driven photoionization. Patel et al. (2015) used  $\text{HS}^-$  as their sulfidic anion, and propose impact-derived sources of metal sulfides (both from the impactor and from subsequent metallogenesis) and evaporatively concentrated iron sulfides as a source for  $\text{HS}^-$ . This postulated mechanism requires specific, local environmental conditions to function. By contrast, simple exposure of a non-acidic lake to the atmosphere anywhere on the planet would supply  $\text{HSO}_3^-$  and  $\text{SO}_3^{2-}$  at prebiotically relevant levels to either supplement the photochemical reducing capacity of  $\text{HS}^-$ , or function as sole sources of hydrated electrons in the Patel et al. (2015) chemistry. Indeed, recent work by the same group suggests that  $\text{HSO}_3^-$  and  $\text{SO}_3^{2-}$  can replace  $\text{HS}^-$  as the source of hydrated electrons upon UV irradiation, and thus drive those parts of the reaction network that do not rely on  $\text{HS}^-$  as a feedstocks (Xu et al. 2017, *in prep*). Reducing or eliminating the dependence of the Patel et al. (2015) chemistry on  $\text{HS}^-$  in favor of  $\text{HSO}_3^-$  or  $\text{SO}_3^{2-}$  increases the robustness of this chemistry, because no special local circumstances need to be invoked. This illustrates how geochemistry can inform improvements of the plausibility of prebiotic pathways.

Indeed, volcanism can be a source of more than sulfidic anions. Volcanism can also be a source of phosphates through partial hydrolysis of volcanically outgassed polyphosphates (Yamagata et al. 1991), and a supplementary source of HCN through photochemical reprocessing of volcanically outgassed reducing species like  $\text{CH}_4$  (Zahnle 1986)<sup>13</sup>. Volcanism could thereby supply or supplement many of the C, H, O, N P & S-containing feedstock molecules and photoreductants required by the Patel et al. (2015) chemistry. The UV light

---

<sup>13</sup>Though some concentration mechanism would be required to achieve prebiotically relevant levels of HCN via this pathway

also required by the Patel et al. (2015) chemistry would be available at Earth’s surface for all but the largest volcanic episodes ( $\phi_S \geq 3 \times 10^{11} \text{ cm}^{-2} \text{ s}^{-1}$ ). Hence, epochs of moderately high volcanism may have been uniquely conducive to cyanosulfidic prebiotic chemistry like that of Patel et al. (2015), especially if they can be adapted to work with  $\text{HSO}_3^-$  or  $\text{SO}_3^{2-}$  instead of  $\text{HS}^-$ .

We considered alternate planetary sources for  $\text{HS}^-$  for the Patel et al. (2015) chemistry. We explored whether shallow hydrothermal systems, such as hot springs, might provide prebiotically-relevant levels of  $\text{HS}^-$ . These sources are high-sulfur systems on modern Earth, and, if shallow, prebiotic chemistry in them might retain access to UV light while accessing high concentrations of sulfidic anions. Surveys of modern hydrothermal systems reveal examples of surficial systems that exhibit micromolar or even millimolar concentrations of  $\text{HS}^-$  (Xu et al. 1998; Vick et al. 2010; Kaasalainen and Stefánsson 2011). However, high concentrations of  $\text{HS}^-$  appear to only be achieved in hot systems<sup>14</sup> ( $T > 60^\circ \text{ C}$ , and typically higher). Similarly, studies of geothermal waters in Yellowstone National Park suggest sulfite availability at the  $0.4 - 5 \mu\text{M}$  level. However, such levels of sulfite were again accessed only in hot waters (Kamyshny et al. 2014). It is not clear how compatible such conditions are with prebiotic chemistry; for example, most of the cyanosulfidic chemistries of Patel et al. (2015) and Xu et al. (2016) were conducted at room temperature ( $25^\circ \text{ C}$ ), and in general many molecules thought to be relevant to the origin of life, such as ribozymes, RNA and their components, are more stable and function better at cooler temperatures (Levy and Miller 1998; Attwater et al. 2010; Kua and Bada 2011; Akoopie and Müller 2016). However, for hot origin-of-life scenarios, hydrothermal systems may be compelling venues for cyanosulfidic reaction networks like that of Patel et al. (2015), reinforcing the utility of volcanism for prebiotic chemistry.

## 6. Conclusion & Next Steps

Constraining the abundances of trace chemical species on early Earth is important to understanding whether postulated prebiotic pathways which are dependent on them could have proceeded. Here, we show that prebiotically-relevant levels of certain sulfidic anions are globally available in shallow, well-mixed aqueous reservoirs due to dissolution of sulfur-bearing gases that are volcanically injected into the atmosphere of early Earth. In particular, anions derived from  $\text{SO}_2$  are available at  $\geq 1 \mu\text{M}$  levels in non-acidic reservoirs for  $\text{SO}_2$  out-

---

<sup>14</sup>We speculate that  $\text{HS}^-$ -rich shallow hydrothermal systems tend to be hot because the same volcanism that supplies elevated levels of  $\text{HS}^-$  also supplies elevated levels of heat.

gassing rates corresponding to the modern Earth and higher. During episodes of intense volcanism, like the emplacement of basaltic fields like the Deccan Traps,  $\text{SO}_2$ -derived anions may be available at  $\geq 1\text{mM}$  levels for reservoirs buffered to  $\text{pH} \geq 7$  (e.g., the modern ocean at  $\text{pH} = 8.2$ ) and at a temperature of  $T = 25^\circ\text{C}$ , though sulfite disproportionation may have ultimately limited concentrations to the  $\sim 10\mu\text{M}$  level; better constraints on sulfite disproportionation reaction rates are required to constrain this possibility. At cooler temperatures, even higher concentrations of these anions would have been available. Formation of mineral precipitate should not inhibit sulfite concentrations until  $\geq 1\text{mM}$  concentrations so long as the reservoir is not acidic, but might suppress sulfite levels in acidic waters. On the other hand, anions derived from  $\text{H}_2\text{S}$  would not have been available at micromolar levels across the plausible range of volcanic outgassing due to low solubility of  $\text{H}_2\text{S}$  and an unfavorable dissociation constant, and prebiotic chemistry invoking such anions must invoke local, specialized sources. Radiative transfer calculations suggests that NUV radiation will remain abundant at the planet surface for  $\phi_S \leq 1 \times 10^{11} \text{ cm}^{-2} \text{ s}^{-1}$ , but will be suppressed for  $\phi_S \geq 3 \times 10^{11} \text{ cm}^{-2} \text{ s}^{-1}$ ; such epochs may be especially clement for surficial, UV-independent prebiotic chemistry. We applied our results to the case study of the proposed prebiotic reaction network of Patel et al. (2015). The prebiotic plausibility of this network can be improved if it can be adapted to use  $\text{SO}_2$ -derived anions like  $\text{HSO}_3^-$  or  $\text{SO}_3^{2-}$  instead of  $\text{HS}^-$ , since the atmosphere is capable of supplying prebiotically-relevant levels of the former directly but more localized sources must be invoked for adequate supply of the latter. Coupled with the potential for volcanogenic synthesis of feedstock molecules like HCN and phosphate (Zahnle 1986; Yamagata et al. 1991), it appears that episodes of moderately intense volcanism ( $\phi_S \approx 1 \times 10^{11} \text{ cm}^{-2} \text{ s}^{-1}$ ) might have been especially clement for cyanosulfidic prebiotic chemistry which exploits  $\text{SO}_2$ -derived anions (e.g.,  $\text{HSO}_3^-$ ). Avenues for future work include simulating these scenarios experimentally and/or with a large general purpose aqueous geochemistry code, improving measurements of the sulfite disproportionation reaction rate constant, and further photochemical modelling to improve constraints on the expected concentrations of  $\text{SO}_2$  and  $\text{H}_2\text{S}$  on early Earth.

## 7. Acknowledgements

We thank A. Levi for his insight regarding equilibrium chemistry, and D. Catling, I. Halevy, M. Claire, J. Szostak, I. Halevy, T. Bosak, and T. Vick for answers to many questions and/or comments on the manuscript. We especially thank J. Toner for extensive discussion and feedback. We thank M. Claire for sharing sulfur aerosol cross-sections for validation purposes. This research has made use of NASA’s Astrophysics Data System Bibliographic Services, and the MPI-Mainz UV-VIS Spectral Atlas of Gaseous Molecules. S. R., Z. R. T.,

D. D. S., and J. D. S. gratefully acknowledge support from the Simons Foundation (S. R., Z. R. T., D. D. S.: grant no. 290360; S.R., grant no. 495062; J. D. S.: grant no. 290362).

## **8. Author Disclosure Statement**

The authors declare no competing financial interests.

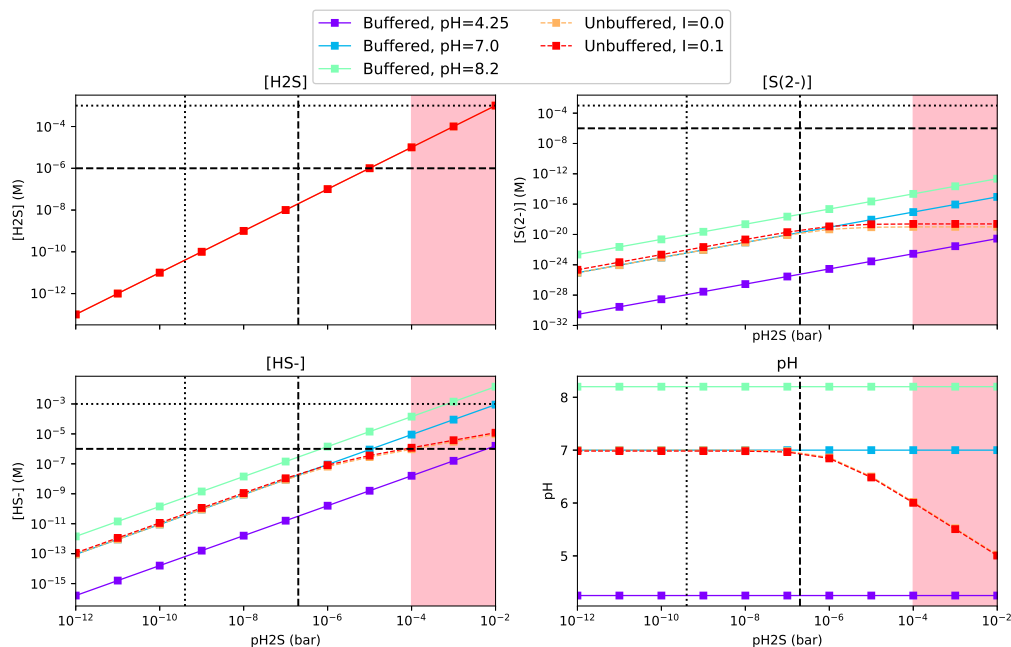


Fig. 1.— Concentrations of sulfur bearing compounds and pH as a function of  $p\text{H}_2\text{S}$  for a well-mixed aqueous reservoir.  $[\text{H}_2\text{S}]$  is calculated from Henry’s Law; the concentrations of  $\text{HS}^-$  and  $\text{S}^{2-}$  are calculated from equilibrium chemistry for 1) solutions buffered to various pHs, and 2) unbuffered solutions with varying ionic strengths. The vertical dotted line demarcates the expected  $p\text{H}_2\text{S}$  for an abiotic Earth with a weakly reducing  $\text{CO}_2\text{-N}_2$  atmosphere with modern levels of sulfur outgassing, from Hu et al. (2013). The vertical dashed line demarcates the expected  $p\text{H}_2\text{S}$  for the same model, but with outgassing levels of sulfur corresponding to the upper limit of the estimate for the emplacement of the terrestrial flood basalts. In the red shaded area,  $p\text{H}_2\text{S}$  is so high it blocks UV light from the planet surface, meaning UV-dependent prebiotic pathways, e.g., those of Patel et al. (2015), cannot function (Ranjan and Sasselov 2017). The red curve largely overplots the orange, demonstrating the minimal impact of ionic strength on the calculation for  $I \leq 0.1$ . The horizontal dashed and dotted lines demarcate micromolar and millimolar concentrations, respectively. The cyanosulfidic chemistry of Patel et al. (2015) has been demonstrated at millimolar S-bearing photoreductant concentrations, and at least high micromolar levels of these compounds are thought to be required for high-yield prebiotic chemistry.

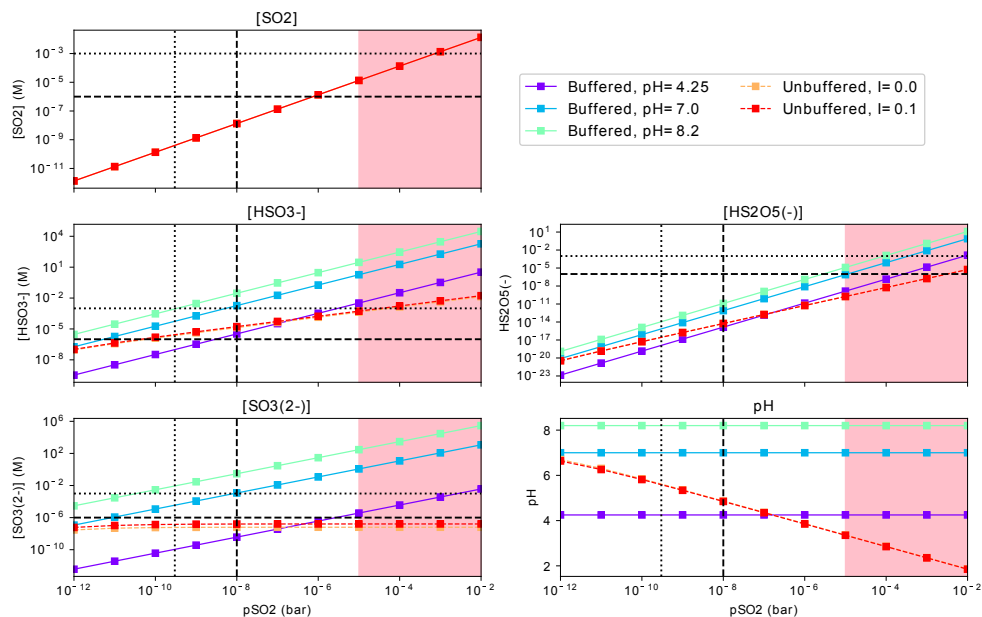


Fig. 2.— Concentrations of sulfur bearing compounds and pH as a function of  $p\text{SO}_2$  for a well-mixed aqueous reservoir.  $[\text{SO}_2]$  is calculated from Henry’s Law; the concentrations of  $\text{HSO}_3^-$ ,  $\text{SO}_3^{2-}$ , and  $\text{HS}_2\text{O}_5^-$  are calculated from equilibrium chemistry for 1) solutions buffered to various pHs, and 2) unbuffered solutions with varying ionic strengths. The vertical dotted line demarcates the expected  $p\text{SO}_2$  for an abiotic Earth with a weakly reducing  $\text{CO}_2\text{-N}_2$  atmosphere with modern levels of sulfur outgassing, from Hu et al. (2013). The vertical dashed line demarcates the expected  $p\text{SO}_2$  for the same model, but with outgassing levels of sulfur corresponding to the upper limit of the estimate for the emplacement of the terrestrial flood basalts. In the red shaded area,  $p\text{SO}_2$  is so high it blocks UV light from the planet surface, meaning UV-dependent prebiotic pathways, e.g., those of Patel et al. (2015), cannot function (Ranjan and Sasselov 2017). The red curve largely overplots the orange, demonstrating the minimal impact of ionic strength on the calculation for  $I \leq 0.1$ . The horizontal dashed and dotted lines demarcate micromolar and millimolar concentrations, respectively. The cyanosulfidic chemistry of Patel et al. (2015) has been demonstrated at millimolar S-bearing photoreductant concentrations, and at least high micromolar levels of these compounds are thought to be required for high-yield prebiotic chemistry.



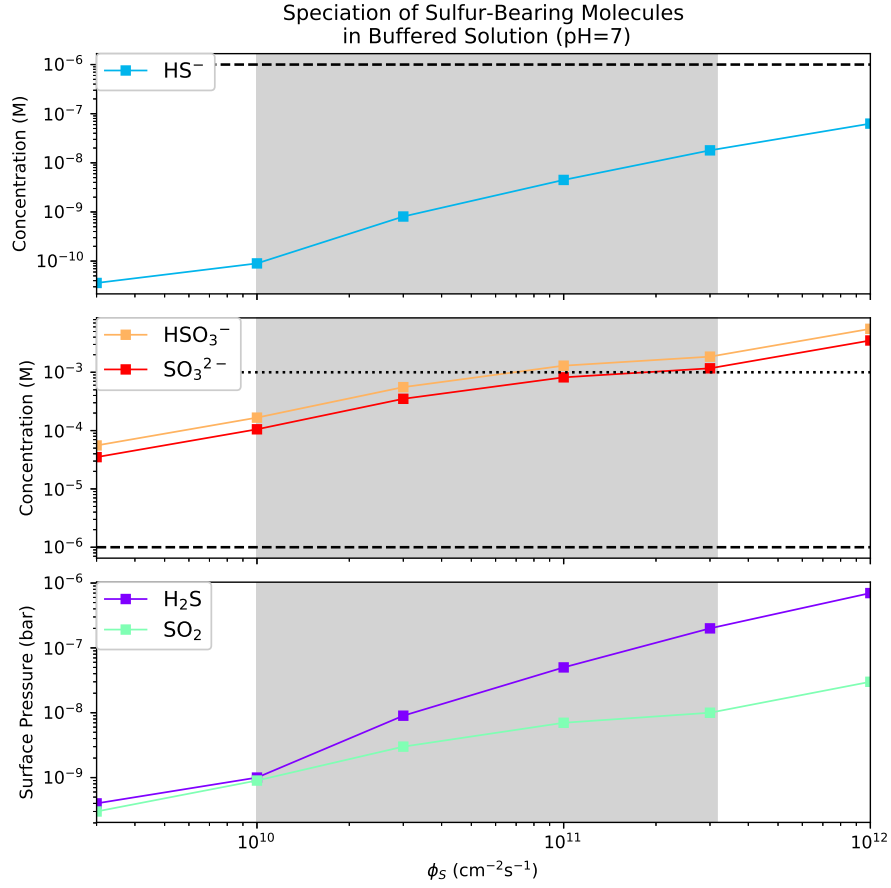


Fig. 3.— Speciation of sulfur-bearing molecules in an aqueous reservoir buffered to pH=7 as a function of total sulfur emission flux  $\phi_S$ . The range of  $\phi_S$  highlighted by Halevy and Head (2014) for emplacement of basaltic plains on Earth is shaded in grey. Horizontal dashed and dotted lines demarcate micromolar and millimolar concentrations, respectively.

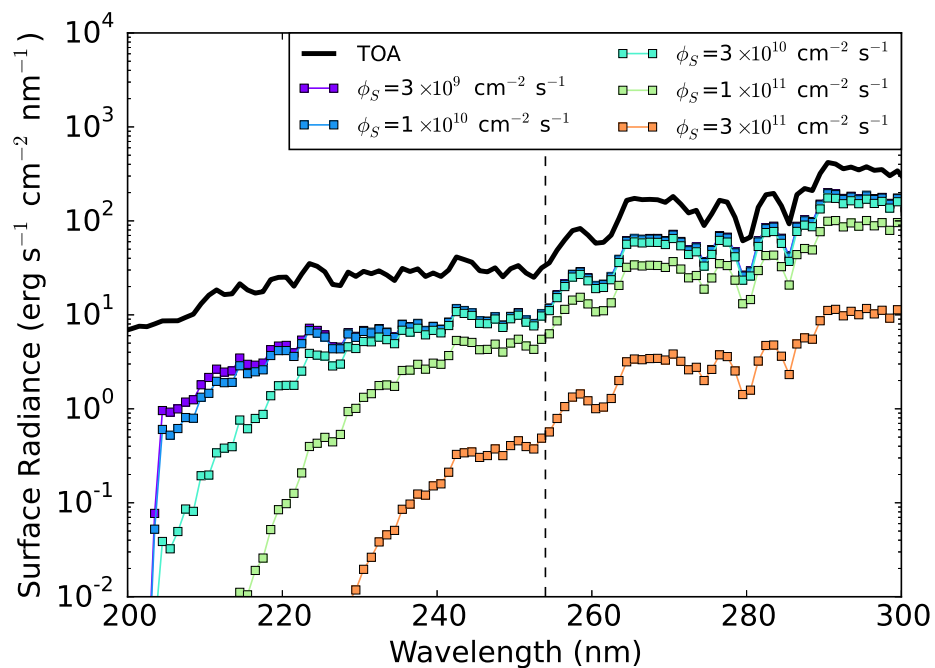


Fig. 4.— UV surface radiance for the early Earth as a function of  $\phi_S$ , using the models of Hu et al. (2013). The black solid line indicates the top-of-atmosphere (TOA) flux, i.e. the irradiation incident at the top of the atmosphere from the young Sun. The vertical dashed line demarcates 254 nm, the wavelength at which the low-pressure mercury lamps commonly used in prebiotic chemistry experiments emit.

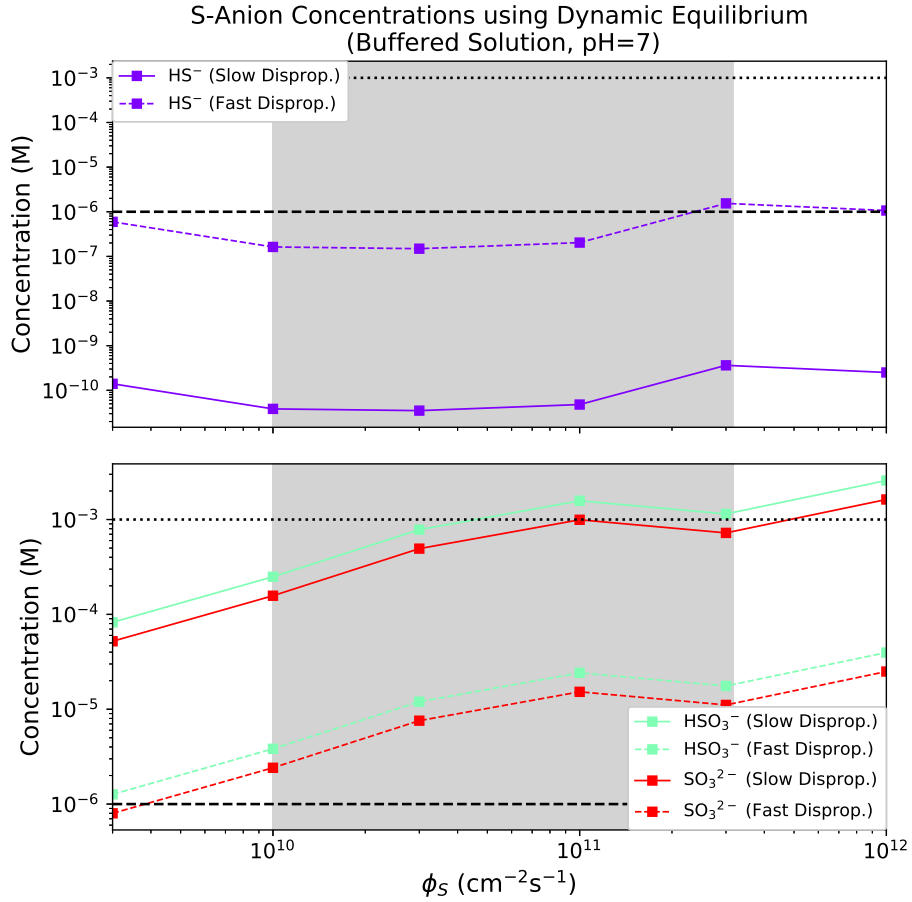


Fig. 5.— Speciation of sulfur-bearing molecules in a shallow lake buffered to pH=7 as a function of total sulfur emission flux  $\phi_S$ , using a dynamic calculation with source atmospheric deposition and sink redox reactions. The range of  $\phi_S$  highlighted by Halevy and Head (2014) for emplacement of basaltic plains on Earth is shaded in grey. Horizontal dashed and dotted lines demarcate micromolar and millimolar concentrations, respectively.  $[\text{HS}^-]$  would not be able to achieve the high concentrations calculated here for the slow disproportionation (low  $k_{17}$ ) case due to solubility constraints.

## REFERENCES

- Akoopie, A. and U. F. Müller (2016). Lower temperature optimum of a smaller, fragmented triphosphorylation ribozyme. *Physical Chemistry Chemical Physics (Incorporating Faraday Transactions)* 18, 20118–20125.
- Amend, J. P. and T. M. McCollom (2009). *Energetics of Biomolecule Synthesis on Early Earth*, Chapter 4, pp. 63–94.
- Amshoff, P., T. Weger, and C. Ostertag-Henning (2016). Kinetics of sulfite disproportionation and thiosulfate acid dissociation. In *Goldschmidt Conference Abstracts*.
- Attwater, J., A. Wochner, V. B. Pinheiro, A. Coulson, and P. Holliger (2010, September). Ice as a protocellular medium for RNA replication. *Nature Communications* 1, 76.
- Bada, J. L., C. Bigham, and S. L. Miller (1994, February). Impact Melting of Frozen Oceans on the Early Earth: Implications for the Origin of Life. *Proceedings of the National Academy of Science* 91, 1248–1250.
- Beckstead, A. A., Y. Zhang, M. S. de Vries, and B. Kohler (2016). Life in the light: nucleic acid photoproperties as a legacy of chemical evolution. *Physical Chemistry Chemical Physics* 18(35), 24228–24238.
- Burkholder, J., J. Abbatt, R. Huie, C. Kolb, V. Orkin, P. Wine, S. Sander, J. Barker, M. Kurylo, and D. Wilmouth (2015). Chemical kinetics and photochemical data for use in atmospheric studies: Evaluation number 18. Technical report, NASA Jet Propulsion Laboratory.
- Claire, M. W., J. F. Kasting, S. D. Domagal-Goldman, E. E. Stüeken, R. Buick, and V. S. Meadows (2014, September). Modeling the signature of sulfur mass-independent fractionation produced in the Archean atmosphere. *Geochimica Cosmochimica Acta* 141, 365–380.
- Claire, M. W., J. Sheets, M. Cohen, I. Ribas, V. S. Meadows, and D. C. Catling (2012, September). The Evolution of Solar Flux from 0.1 nm to 160  $\mu\text{m}$ : Quantitative Estimates for Planetary Studies. *Astrophysical Journal* 757, 95.
- Cockell, C. S. (2000, February). The ultraviolet history of the terrestrial planets - implications for biological evolution. *Planet. Space Sci.* 48, 203–214.
- Coderre, F. and D. G. Dixon (1999). Modeling the cyanide heap leaching of cupriferous gold ores: Part 1: Introduction and interpretation of laboratory column leaching data. *Hydrometallurgy* 52(2), 151–175.

- Corliss, J. B., J. Baross, and S. Hoffman (1981). An hypothesis concerning the relationships between submarine hot springs and the origin of life on earth. *Oceanologica Acta, Special issue Special Issue*.
- Crespo-Hernández, C. E., B. Cohen, P. M. Hare, and B. Kohler (2004). Ultrafast excited-state dynamics in nucleic acids. *Chemical reviews* 104(4), 1977–2020.
- Cronin, T. W. (2014, August). On the Choice of Average Solar Zenith Angle. *Journal of Atmospheric Sciences* 71, 2994–3003.
- Deamer, D. and B. Damer (2017). Can life begin on enceladus? a perspective from hydrothermal chemistry. *Astrobiology*.
- Deamer, D. W. and P. Dworkin, J (2005). *Prebiotic Chemistry*. Springer.
- Debye, P. and E. Huckel (1923). On the Theory of Electrolytes. I. Freezing point depression and related phenomena. *Physik Z* 24, 185–206.
- Delano, J. W. (2001, August). Redox History of the Earth’s Interior since ~3900 Ma: Implications for Prebiotic Molecules. *Origins of Life and Evolution of the Biosphere* 31, 311–341.
- Farquhar, J., H. Bao, and M. Thiemens (2000, August). Atmospheric Influence of Earth’s Earliest Sulfur Cycle. *Science* 289, 756–759.
- Farquhar, J., J. Savarino, S. Airieau, and M. H. Thiemens (2001, December). Observation of wavelength-sensitive mass-independent sulfur isotope effects during SO<sub>2</sub> photolysis: Implications for the early atmosphere. *Journal of Geophysical Research* 106, 32829–32840.
- Forsythe, J. G., S.-S. Yu, I. Mamajanov, M. A. Grover, R. Krishnamurthy, F. M. Fernández, and N. V. Hud (2015). Ester-mediated amide bond formation driven by wet–dry cycles: A possible path to polypeptides on the prebiotic earth. *Angewandte Chemie International Edition* 54(34), 9871–9875.
- Grant, W. and B. Jones (2000). *Alkaline environments*, Volume 1, pp. 126–133. Academic Press, London and New York.
- Guekezian, M., N. Coichev, M. E. V. Suarez-Iha, and E. de Almeida Neves (1997). Stability of sulfur(iv) solutions in the presence of amines and the tendency of sulfite ions to disproportionate in stock solutions. *Analytical Letters* 30(7), 1423–1436.

- Halevy, I. (2013, October). Production, preservation, and biological processing of mass-independent sulfur isotope fractionation in the Archean surface environment. *Proceedings of the National Academy of Science* 110, 17644–17649.
- Halevy, I. and A. Bachan (2017, March). The geologic history of seawater pH. *Science* 355, 1069–1071.
- Halevy, I. and J. W. Head, III (2014, December). Episodic warming of early Mars by punctuated volcanism. *Nature Geoscience* 7, 865–868.
- Halevy, I., M. T. Zuber, and D. P. Schrag (2007, December). A Sulfur Dioxide Climate Feedback on Early Mars. *Science* 318, 1903–.
- Hall-Spencer, J. M., R. Rodolfo-Metalpa, S. Martin, E. Ransome, M. Fine, S. M. Turner, S. J. Rowley, D. Tedesco, and M.-C. Buia (2008, July). Volcanic carbon dioxide vents show ecosystem effects of ocean acidification. *Nature* 454, 96–99.
- Halmer, M. M., H.-U. Schmincke, and H.-F. Graf (2002, June). The annual volcanic gas input into the atmosphere, in particular into the stratosphere: a global data set for the past 100 years. *Journal of Volcanology and Geothermal Research* 115, 511–528.
- He, C., I. Gállego, B. Laughlin, M. A. Grover, and N. V. Hud (2017). A viscous solvent enables information transfer from gene-length nucleic acids in a model prebiotic replication cycle. *Nature Chemistry* 9(4), 318–324.
- Higgs, P. G. and N. Lehman (2015). The rna world: molecular cooperation at the origins of life. *Nature Reviews Genetics* 16(1), 7–17.
- Holm, N. G. and J. L. Charlou (2001, August). Initial indications of abiotic formation of hydrocarbons in the Rainbow ultramafic hydrothermal system, Mid-Atlantic Ridge. *Earth and Planetary Science Letters* 191, 1–8.
- Hu, R., S. Seager, and W. Bains (2013, May). Photochemistry in Terrestrial Exoplanet Atmospheres. II. H<sub>2</sub>S and SO<sub>2</sub> Photochemistry in Anoxic Atmospheres. *Astrophysical Journal* 769, 6.
- Kaasalainen, H. and A. Stefánsson (2011, May). Sulfur speciation in natural hydrothermal waters, Iceland. *Geochimica Cosmochimica Acta* 75, 2777–2791.
- Kamyshny, A., G. Druschel, Z. F. Mansaray, and J. Farquhar (2014, May). Multiple sulfur isotopes fractionations associated with abiotic sulfur transformations in yellowstone national park geothermal springs. *Geochemical Transactions* 15(1), 7.

- Kasting, J. F. (1987). Theoretical constraints on oxygen and carbon dioxide concentrations in the precambrian atmosphere. *Precambrian research* 34(3), 205–229.
- Kasting, J. F. (1993, February). Earth’s early atmosphere. *Science* 259, 920–926.
- Kasting, J. F. (2014). Atmospheric composition of hadean–early archean earth: The importance of co. *Geological Society of America Special Papers* 504, 19–28.
- Kasting, J. F. and J. C. G. Walker (1981, February). Limits on oxygen concentration in the prebiological atmosphere and the rate of abiotic fixation of nitrogen. *J. Geophys. Res.* 86, 1147–1158.
- Kasting, J. F., K. J. Zahnle, J. P. Pinto, and A. T. Young (1989, March). Sulfur, ultraviolet radiation, and the early evolution of life. *Origins of Life and Evolution of the Biosphere* 19, 95–108.
- Kua, J. and J. L. Bada (2011, December). Primordial Ocean Chemistry and its Compatibility with the RNA World. *Origins of Life and Evolution of the Biosphere* 41, 553–558.
- Larowe, D. E. and P. Regnier (2008, October). Thermodynamic Potential for the Abiotic Synthesis of Adenine, Cytosine, Guanine, Thymine, Uracil, Ribose, and Deoxyribose in Hydrothermal Systems. *Origins of Life and Evolution of the Biosphere* 38, 383–397.
- Lerman, A., D. Imboden, and J. Gat (Eds.) (1995). *Physics and Chemistry of Lakes, Second Edition*. Springer-Verlag.
- Levy, M. and S. L. Miller (1998, July). The Stability of the RNA Bases: Implications for the Origin of Life. *Proceedings of the National Academy of Science* 95, 7933–7938.
- Li, W., A. D. Czaja, M. J. Van Kranendonk, B. L. Beard, E. E. Roden, and C. M. Johnson (2013, November). An anoxic, Fe(II)-rich, U-poor ocean 3.46 billion years ago. *Geochimica Cosmochimica Acta* 120, 65–79.
- Lide, D. R. (Ed.) (2009). *CRC Handbook of Chemistry and Physics* (90 ed.). Boca Raton, FL: CRC Press.
- Löhr, A., T. Bogaard, A. Heikens, M. Hendriks, S. Sumarti, M. v. Bergen, K. C. v. Gestel, N. v. Straalen, P. Vroon, and B. Widianarko (2005). Natural pollution caused by the extremely acid crater lake kawah ijen, east java, indonesia (7 pp). *Environmental Science and Pollution Research* 12(2), 89–95.
- Martin, W., J. Baross, D. Kelley, and M. J. Russell (2008). Hydrothermal vents and the origin of life. *Nature Reviews Microbiology* 6(11), 805–814.

- Maurer, S. E. and G. Nguyen (2016). Prebiotic vesicle formation and the necessity of salts. *Origins of Life and Evolution of Biospheres* 46(2-3), 215–222.
- McCollom, T. M. (2013, May). Miller-Urey and Beyond: What Have We Learned About Prebiotic Organic Synthesis Reactions in the Past 60 Years? *Annual Review of Earth and Planetary Sciences* 41, 207–229.
- McCollom, T. M. and J. S. Seewald (2007). Abiotic synthesis of organic compounds in deep-sea hydrothermal environments. *Chemical Reviews* 107(2), 382–401.
- Meyer, B., M. Rigdon, T. Burner, M. Ospina, K. Ward, and K. Koshlap (1982). *Thermal Decomposition of Sulfite, Bisulfite, and Disulfite Solutions*, Chapter 6, pp. 113–125. American Chemical Society.
- Mirzoyan, N. and I. Halevy (2014). Kinetics of sulfite disproportionation and thiosulfate acid dissociation. In *Goldschmidt Conference Abstracts*.
- Misra, K. C. (2012). *Introduction to Geochemistry*. Wiley-Blackwell.
- Mojzsis, S. J., T. M. Harrison, and R. T. Pidgeon (2001, January). Oxygen-isotope evidence from ancient zircons for liquid water at the Earth’s surface 4,300Myr ago. *Nature* 409, 178–181.
- Morse, J. W. and F. T. Mackenzie (1998, Sep). Hadean ocean carbonate geochemistry. *Aquatic Geochemistry* 4(3), 301–319.
- Mulkidjanian, A. Y., A. Y. Bychkov, D. V. Dibrova, M. Y. Galperin, and E. V. Koonin (2012, April). PNAS Plus: Origin of first cells at terrestrial, anoxic geothermal fields. *Proceedings of the National Academy of Science* 109, E821–E830.
- Mulkidjanian, A. Y., D. A. Cherepanov, and M. Y. Galperin (2003). Survival of the fittest before the beginning of life: selection of the first oligonucleotide-like polymers by uv light. *BMC evolutionary biology* 3, 12.
- Mutschler, H., A. Wochner, and P. Holliger (2015). Freeze–thaw cycles as drivers of complex ribozyme assembly. *Nature chemistry* 7(6), 502–508.
- Neta, P. and R. E. Huie (1985). Free-radical chemistry of sulfite. *Environmental health perspectives* 64, 209.
- Novoselov, A. A., D. Silva, J. Schneider, X. C. Abrevaya, M. S. Chaffin, P. Serrano, M. S. Navarro, M. J. Conti, and C. R. d. Souza Filho (2017, June). Geochemical constraints on the Hadean environment from mineral fingerprints of prokaryotes. *Scientific Reports* 7, 4008.



- Parkhurst, D. L. and C. A. J. Appelo (2013). Description of input and examples for phreeqc version 3: A computer program for speciation, batch-reaction, one-dimensional transport, and inverse geochemical calculations. Technical report, U. S. Geological Survey. Chapter 43 of Section A: Groundwater in Book 6 Modeling Techniques.
- Pascal, R. (2012). Suitable energetic conditions for dynamic chemical complexity and the living state. *Journal of Systems Chemistry* 3(1), 1.
- Patel, B. H., C. Percivalle, D. J. Ritson, C. D. Duffy, and J. D. Sutherland (2015, April). Common origins of RNA, protein and lipid precursors in a cyanosulfidic protometabolism. *Nature Chemistry* 7, 301–307.
- Pavlov, A. A. and J. F. Kasting (2002, March). Mass-Independent Fractionation of Sulfur Isotopes in Archean Sediments: Strong Evidence for an Anoxic Archean Atmosphere. *Astrobiology* 2, 27–41.
- Pollum, M., B. Ashwood, S. Jockusch, M. Lam, and C. E. Crespo-Hernández (2016). Unintended consequences of expanding the genetic alphabet. *Journal of the American Chemical Society* 138(36), 11457–11460.
- Powner, M. W., B. Gerland, and J. D. Sutherland (2009). Synthesis of activated pyrimidine ribonucleotides in prebiotically plausible conditions. *Nature* 459(7244), 239–242.
- Ranjan, S. and D. D. Sasselov (2016, January). Influence of the UV Environment on the Synthesis of Prebiotic Molecules. *Astrobiology* 16, 68–88.
- Ranjan, S. and D. D. Sasselov (2017, March). Constraints on the Early Terrestrial Surface UV Environment Relevant to Prebiotic Chemistry. *Astrobiology* 17, 169–204.
- Ranjan, S., R. Wordsworth, and D. D. Sasselov (2017). Atmospheric Constraints on the Surface UV Environment of Mars at 3.9 Ga Relevant to Prebiotic Chemistry. *Astrobiology* 17, 687–708.
- Rapf, R. J. and V. Vaida (2016). Sunlight as an energetic driver in the synthesis of molecules necessary for life. *Phys. Chem. Chem. Phys.* 18, 20067–20084.
- Richter, F. M. (1985, May). Models for the Archean thermal regime. *Earth and Planetary Science Letters* 73, 350–360.
- Rickard, D. and G. W. Luther (2007). Chemistry of iron sulfides. *Chemical reviews* 107(2), 514–562.

- Rios, A. C. and Y. Tor (2013). On the origin of the canonical nucleobases: An assessment of selection pressures across chemical and early biological evolution. *Israel journal of chemistry* 53(6-7), 469–483.
- Ritson, D. and J. D. Sutherland (2012, November). Prebiotic synthesis of simple sugars by photoredox systems chemistry. *Nature Chemistry* 4, 895–899.
- Robock, A. (2000, May). Volcanic eruptions and climate. *Reviews of Geophysics* 38, 191–219.
- Rugheimer, S., A. Segura, L. Kaltenegger, and D. Sasselov (2015, June). UV Surface Environment of Earth-like Planets Orbiting FGKM Stars through Geological Evolution. *Astrophysical Journal* 806, 137.
- Ruiz-Mirazo, K., C. Briones, and A. de la Escosura (2014). Prebiotic systems chemistry: new perspectives for the origins of life. *Chem. Rev* 114(1), 285–366.
- Rumble, J. R. (Ed.) (2017). *CRC Handbook of Chemistry and Physics* (98 ed.). Boca Raton, FL: CRC Press.
- Sagan, C. (1973). Ultraviolet selection pressure on the earliest organisms. *Journal of Theoretical Biology* 39, 195–200.
- Sagan, C. and B. N. Khare (1971, July). Long-Wavelength Ultraviolet Photoproduction of Amino Acids on the Primitive Earth. *Science* 173, 417–420.
- Sander, R. (2015, April). Compilation of Henry’s law constants (version 4.0) for water as solvent. *Atmospheric Chemistry & Physics* 15, 4399–4981.
- Sarker, P. K., J.-i. Takahashi, Y. Obayashi, T. Kaneko, and K. Kobayashi (2013, June). Photo-alteration of hydantoins against UV light and its relevance to prebiotic chemistry. *Advances in Space Research* 51, 2235–2240.
- Segura, A., K. Krelove, J. F. Kasting, D. Sommerlatt, V. Meadows, D. Crisp, M. Cohen, and E. Mlawer (2003, December). Ozone Concentrations and Ultraviolet Fluxes on Earth-Like Planets Around Other Stars. *Astrobiology* 3, 689–708.
- Self, S., M. Widdowson, T. Thordarson, and A. E. Jay (2006, August). Volatile fluxes during flood basalt eruptions and potential effects on the global environment: A Deccan perspective. *Earth and Planetary Science Letters* 248, 518–532.
- Serrano-Andres, L. and M. Merchan (2009). Are the five natural dna/rna base monomers a good choice from natural selection?: A photochemical perspective. *Journal of Photochemistry and Photobiology C: Photochemistry Reviews* 10(1), 21–32.

- Siu, T. and C. Q. Jia (1999). Kinetic and mechanistic study of reaction between sulfide and sulfite in aqueous solution. *Industrial & engineering chemistry research* 38(10), 3812–3816.
- Sojo, V., B. Herschy, A. Whicher, E. Camprubí, and N. Lane (2016, February). The Origin of Life in Alkaline Hydrothermal Vents. *Astrobiology* 16, 181–197.
- Šponer, J. E., R. Szabla, R. W. Góra, A. M. Saitta, F. Pietrucci, F. Saija, E. Di Mauro, R. Saladino, M. Ferus, S. Civiš, et al. (2016). Prebiotic synthesis of nucleic acids and their building blocks at the atomic level—merging models and mechanisms from advanced computations and experiments. *Physical Chemistry Chemical Physics* 18(30), 20047–20066.
- Springsteen, G. (2015). Reaching back to jump forward: Recent efforts towards a systems-level hypothesis for an early rna world. *ChemBioChem* 16, 1411–1413.
- Taylor, L. L., S. A. Banwart, P. J. Valdes, J. R. Leake, and D. J. Beerling (2012). Evaluating the effects of terrestrial ecosystems, climate and carbon dioxide on weathering over geological time: a global-scale process-based approach. *Philosophical Transactions of the Royal Society of London B: Biological Sciences* 367(1588), 565–582.
- Trail, D., E. B. Watson, and N. D. Tailby (2011, December). The oxidation state of Hadean magmas and implications for early Earth’s atmosphere. *Nature* 480, 79–82.
- Truesdell, A. H. and B. F. Jones (1974, April). WATEQ, A Computer Program for Calculating Chemical Equilibria of Natural Water. *Journal Research U.S. Geological Survey* 2, 233–248.
- Urey, H. C. (1952, April). On the Early Chemical History of the Earth and the Origin of Life. *Proceedings of the National Academy of Science* 38, 351–363.
- Vick, T., J. A. Dodsworth, K. Costa, E. Shock, and B. P. Hedlund (2010). Microbiology and geochemistry of little hot creek, a hot spring environment in the long valley caldera. *Geobiology* 8(2), 140–154.
- Walker, S. I., M. A. Grover, and N. V. Hud (2012, April). Universal Sequence Replication, Reversible Polymerization and Early Functional Biopolymers: A Model for the Initiation of Prebiotic Sequence Evolution. *PLoS ONE* 7, e34166.
- Watmough, S. A. and J. Aherne (2008). Estimating calcium weathering rates and future lake calcium concentrations in the muskoka–haliburton region of ontario. *Canadian Journal of Fisheries and Aquatic Sciences* 65(5), 821–833.

- Wordsworth, R. and R. Pierrehumbert (2013, January). Hydrogen-Nitrogen Greenhouse Warming in Earth’s Early Atmosphere. *Science* 339, 64.
- Xu, J., D. J. Ritson, S. Ranjan, D. D. Sasselov, and J. S. Sutherland (2017, March). Photochemical reductive homologation of nitriles using bisulfite/sulfite as the source of hydrated electrons. in prep.
- Xu, J., M. Tsanakopoulou, C. J. Magnani, R. Szabla, J. E. Šponer, J. Šponer, R. W. Góra, and J. D. Sutherland (2016). A prebiotically plausible synthesis of pyrimidine  $\beta$ -ribonucleosides and their phosphate derivatives involving photoanomerization. *Nature Chemistry*.
- Xu, Y., M. A. A. Schoonen, D. K. Nordstrom, K. M. Cunningham, and J. W. Ball (1998, December). Sulfur geochemistry of hydrothermal waters in Yellowstone National Park: I. the origin of thiosulfate in hot spring waters. *Geochimica Cosmochimica Acta* 62, 3729–3743.
- Yamagata, Y., H. Watanabe, et al. (1991). Volcanic production of polyphosphates and its relevance to prebiotic evolution. *Nature* 352(6335), 516.
- Zahnle, K., M. Claire, and D. Catling (2006). The loss of mass-independent fractionation in sulfur due to a palaeoproterozoic collapse of atmospheric methane. *Geobiology* 4(4), 271–283.
- Zahnle, K. J. (1986, February). Photochemistry of methane and the formation of hydrocyanic acid (HCN) in the Earth’s early atmosphere. *Journal of Geophysical Research* 91, 2819–2834.
- Zeebe, R. E. and D. A. Wolf-Gladrow (2009). *Carbon Dioxide, Dissolved (Ocean)*, pp. 123–127. Dordrecht: Springer Netherlands.

### A. Atmospheric Sulfur Speciation

We use the work of Hu et al. (2013) to connect the sulfur emission flux  $\phi_S$  to the speciation of atmospheric sulfur. Table 2 presents H<sub>2</sub>S and SO<sub>2</sub> mixing ratios as a function of  $\phi_S$  from Hu et al. (2013) (their Fig. 5, CO<sub>2</sub>-dominated atmosphere case).

Table 2: Column-integrated mixing ratios of H<sub>2</sub>S and SO<sub>2</sub> as a function of  $\phi_S$  from Hu et al. (2013) (their Fig. 5, CO<sub>2</sub>-dominated case).

$\phi_S$ (cm <sup>-2</sup> s <sup>-1</sup> )	$r_{H_2S}$	$r_{SO_2}$
$3 \times 10^9$	$4 \times 10^{-10}$	$3 \times 10^{-10}$
$1 \times 10^{10}$	$1 \times 10^{-9}$	$9 \times 10^{-10}$
$3 \times 10^{10}$	$9 \times 10^{-9}$	$3 \times 10^{-9}$
$1 \times 10^{11}$	$5 \times 10^{-8}$	$7 \times 10^{-9}$
$3 \times 10^{11}$	$2 \times 10^{-7}$	$1 \times 10^{-8}$
$1 \times 10^{12}$	$7 \times 10^{-7}$	$3 \times 10^{-8}$
$3 \times 10^{12}$	$2 \times 10^{-6}$	$8 \times 10^{-8}$
$1 \times 10^{13}$	$9 \times 10^{-6}$	$3 \times 10^{-7}$

### B. Activity Coefficient Calculation

This appendix describes the calculation of the activity coefficients of the ions involved in equilibria reactions for SO<sub>2</sub> and H<sub>2</sub>S.

We use the Extended Debye-Huckel (EDH) Theory to calculate activity coefficients ( $\gamma_i$ ) for the ions in our study. EDH is valid for ionic strengths up to 0.1M, which is the highest ionic strength we consider, motivated by the fact that lipid vesicle formation is inhibited at ionic strengths above 0.1M (Maurer and Nguyen 2016).

Extended Debye Huckel theory states that:

$$\log \gamma_i = -Az_i^2 \frac{I^{0.5}}{1 + B\alpha_i I^{0.5}} \quad (\text{B1})$$

where  $A$  and  $B$  depend on the temperature, density, and dielectric constant of the solvent (in our case water), and  $\alpha_i$  is an ion-specific parameter. We took  $A = 0.5085 \text{ M}^{-1/2}$  and  $B = 0.3281 \text{ M}^{-1/2} \text{ \AA}^{-1}$ , corresponding to  $T = 25^\circ\text{C}$ ; Appendix D describes the sensitivity of our analysis to this assumption. Table 3 summarizes the  $\alpha_i$  used in our study, taken from Misra (2012). We were unable to locate a value of  $\alpha_C$  for HS<sub>2</sub>O<sub>5</sub><sup>-</sup>, and consequently take

$\gamma_{HS_2O_5^-} = 1$  throughout (i.e., we do not correct for its activity). Since in our analysis the supply of  $SO_2$  is not limited (the atmosphere is treated as an infinite reservoir),  $pK_{aSO_2,3}$  affects only the abundance of  $H_2SO_5^-$ , which is a trace compound in our analysis (see Fig. 2).

Table 3: Values for the ion-specific parameter  $\alpha$  (related to the hydration sphere of the ion) used to calculate activity coefficients.

Ion	$\alpha_i(\text{\AA})$
$HSO_3^-$	4.0
$SO_3^{2-}$	4.5
$HS^-$	3.5
$S^{2-}$	5.0
$OH^-$	3.5
$H^+$	9.0

Table 4 shows the activity coefficients for the relevant ions at the two ionic strengths considered in our study:

Table 4: Per-ion activity coefficients for different ionic strengths.

Ion	I=0 M	I=0.1 M
$HSO_3^-$	1.0	0.770
$SO_3^{2-}$	1.0	0.364
$HS^-$	1.0	0.762
$S^{2-}$	1.0	0.377
$OH^-$	1.0	0.762
$H^+$	1.0	0.826

### C. Sensitivity of Henry’s Law Constants to Salinity

This appendix describes our assessment of the sensitivity of the Henry’s Law coefficients for  $SO_2$  and  $H_2S$  to salinity.

We account for the effect of salinity on  $H_G$  using the Schumpe-Sechenov method, as outlined in Burkholder et al. (2015):

$$\log H_0/H = \sum_i (h_i + h_G) * c_i, \tag{C1}$$

where  $H_0$  is the Henry’s Law constant in pure water,  $H$  is the Henry’s law constant in saline solution,  $c_i$  is the concentration of the ion  $i$ ,  $h_i$  is an ion-specific constant, and  $h_G$  is a gas-specific constant.  $h_G$  is temperature dependent, via  $h_G = h_0 + h_T(T - 298.15K)$ . NaCl is the dominant salt in Earth’s oceans; we approximate NaCl as the sole source of salinity in our calculations. Table 5 summarizes the values of these parameters used for this study, all taken from the compendium of Burkholder et al. (2015). We were unable to locate a value for  $h_T$  for H<sub>2</sub>S in our literature search, and assumed  $h_T = 0$  for this case.

Table 5: Parameters used to estimate the dependence of Henry’s Law constants on [NaCl].

Parameter	H <sub>2</sub> S	SO <sub>2</sub>	Na <sup>+</sup>	Cl <sup>-</sup>
$H_0$ (M/bar)	0.101	1.34	–	–
$h_0$ (M <sup>-1</sup> )	-0.0333	-0.0607	–	–
$h_T$ (M <sup>-1</sup> )	0 <sup>a</sup>	0.000275	–	–
$h_i$ (M <sup>-1</sup> )	–	–	0.1143	0.0318

The Henry’s Law constants for these gases as a function of [NaCl] at  $T = 298.15K$  is show in Fig. 6. In this study, we consider ionic strengths  $I \leq 0.1M$ , corresponding to  $[NaCl] \leq 0.1M$ . At such levels, salinity has a negligible effect on Henry’s Law solubility, and we consequently neglect it in our calculations.

## D. Sensitivity of Analysis to Temperature

This appendix describes our assessment of the sensitivity of our calculations to the temperature of the aqueous reservoir in which the equilibrium chemistry proceeds.

### D.1. Sensitivity of Henry’s Law Constants to Temperature

We calculated the effect of temperature on Henry’s Law using the three-term empirical fit outlined in Burkholder et al. (2015), i.e.  $\ln(H) = A + B/T + C \ln(T)$ , where  $H$  is in units of M/atm and  $A$ ,  $B$ , and  $C$  are gas-specific coefficients of an empirical fit. The values of these coefficients for H<sub>2</sub>S and SO<sub>2</sub> were taken from Burkholder et al. (2015) and are summarized in Table 6.  $H(T)$  for H<sub>2</sub>S and SO<sub>2</sub> is plotted in Fig. 7. For temperatures ranging from 0 – 50° (273.15 – 323.15 K), the Henry’s Law constants vary by less than a factor of 2.5 relative to their values at 25°C (293.15K), which is small compared to the order-of-magnitude variations in concentration we focus on in this study. We also estimated the temperature dependence

using the van’t Hoff equation as outlined in Sander (2015), and obtained similar results.

Table 6: Parameters used to estimate dependence of Henry’s Law constant on temperature

Parameter	H <sub>2</sub> S	SO <sub>2</sub>
<i>A</i>	-145.2	-39.72
<i>B</i>	8120	4250
<i>C</i>	20.296	4.525

### D.2. Sensitivity of Reaction Rates to Temperature

In order to assess the temperature dependence of acid dissociation pKa’s, we use the Van’t Hoff Equation:

$$\frac{\partial[\ln K_0]}{\partial T} = \frac{\Delta H_0}{RT^2} \tag{D1}$$

Where  $K_0$  is the equilibrium constant,  $T$  is temperature,  $\Delta H_0$  is the change in enthalpy, and  $R = 8.314 \times 10^{-3} \text{kJ/mol/K}$ . Solving this differential equation, assuming temperature-invariant enthalpy of solution<sup>15</sup>, gives:

$$\ln(K_2) = \ln(K_1) + \frac{-\Delta H_0}{R} \left( \frac{1}{T_2} - \frac{1}{T_1} \right) \tag{D2}$$

With this equation, the acid dissociation constant  $K_2$  can be estimated at a given temperature  $T_2$ , provided its value  $K_1$  is known at a reference temperature  $T_1$ .  $\Delta H$  is the change in enthalpy of the reaction, given by:

$$\Delta H = \sum \Delta H_f^\circ(\text{products}) - \sum \Delta H_f^\circ(\text{reactants}) \tag{D3}$$

The enthalpies of formation for the products and reactants of the first two acid dissociation reactions for H<sub>2</sub>S and SO<sub>2</sub> are taken from Lide (2009), and are shown in Table 7. Note that  $\Delta H_f^\circ = 0$  for H<sup>+</sup>, by definition. We were unable to locate an enthalpy of formation for

---

<sup>15</sup>We expect this assumption to be reasonable because of the limited range of temperatures that are plausible for our surface aqueous reservoir scenario.



$\text{H}_2\text{SO}_5^-$ , and consequently are unable to calculate the temperature-dependence of  $\text{pK}_{\text{a}_{\text{SO}_2,3}}$ . Since in our analysis the supply of  $\text{SO}_2$  is not limited (the atmosphere is treated as an infinite reservoir),  $\text{pK}_{\text{a}_{\text{SO}_2,3}}$  affects only the abundance of  $\text{H}_2\text{SO}_5^-$ , which is a trace compound in our analysis (see Fig. 2).

Table 7: Enthalpies of formation used in the Van’t Hoff Equation calculation.

Molecule	$\Delta H_f^\circ$ (kJ/mol)
$\text{HSO}_3^-$	-626.2
$\text{SO}_3^{2-}$	-635.5
$\text{SO}_2$	-296.8
$\text{HS}^-$	-17.6
$\text{S}^{2-}$	33.1
$\text{H}_2\text{S}$	-20.6
$\text{H}_2\text{O}$	-285.8

Using these values and the Van’t Hoff equation, we calculated the temperature dependence of the first two acid dissociation constants for aqueous  $\text{H}_2\text{S}$  and  $\text{SO}_2$ . Table 8 shows these  $\text{pK}_a$ ’s for  $\text{SO}_2$  and  $\text{H}_2\text{S}$  at 0, 25, and 50°C.

Table 8:  $\text{pK}_a$  at temperatures of 0°C, 25°C, and 50°C and reaction enthalpies

	T=0 ° C	T=25 ° C	T=50 ° C	$\Delta H_{rxn}^\circ$ (kJ/mol)
$\text{H}_2\text{S}, \text{pK}_{a_1}$	7.098	7.05	7.009	3.0
$\text{H}_2\text{S}, \text{pK}_{a_2}$	19.81	19.0	18.31	50.7
$\text{SO}_2, \text{pK}_{a_1}$	1.160	1.86	2.452	-43.6
$\text{SO}_2, \text{pK}_{a_2}$	7.051	7.2	7.326	-9.3

The variation in  $\text{pK}_a$  is negligible for all reactions except the first dissociation of  $\text{SO}_2$ ;  $\text{pK}_{\text{a}_{\text{SO}_2,1}}$  increases significantly with temperature. This implies that in non-acidic solutions, the concentrations of  $\text{SO}_2$ -derived anions should decrease, and conversely that as temperature decreases they should increase.

### D.3. Sensitivity of Activity Coefficients to Temperature

Temperature dependence enters the calculation of the activity coefficients through the parameters  $A$  and  $B$  (see Appendix B for details). For water, at  $T = 0^\circ\text{C}$ ,  $A = 0.4883 \text{ M}^{-1/2}$

and  $B = 0.3241 \text{ M}^{-1/2} \text{ \AA}^{-1}$ ; at  $T = 25^\circ\text{C}$ ,  $A = 0.5085 \text{ M}^{-1/2}$  and  $B = 0.3281 \text{ M}^{-1/2} \text{ \AA}^{-1}$ ; and at  $T = 50^\circ\text{C}$ ,  $A = 0.5319 \text{ M}^{-1/2}$  and  $B = 0.3321 \text{ M}^{-1/2} \text{ \AA}^{-1}$  (Misra 2012). From  $T = 0\text{--}50^\circ\text{C}$ , the activity coefficients varied by  $< 8\%$  for  $I \leq 0.1$ .

#### D.4. Overall Sensitivity of Analysis to Temperature

We evaluated the overall sensitivity of our analysis to our assumption of  $T = 25^\circ\text{C}$  by repeating our analysis at  $T = 0^\circ$  and  $T = 50^\circ$ , and including the effects of temperature on Henry’s Law constant, the reaction pKa’s, and the activity coefficients, simultaneously. Across the tested range, temperature had a negligible impact on the abundances of the  $\text{H}_2\text{S}$ -derived anions, but a significant impact on the abundances of the  $\text{SO}_2$ -derived anions.  $H_{\text{SO}_2}$  decreases with temperature, and  $\text{pKa}_{\text{SO}_2,1}$  increases with temperature; both effects serve to increase the concentration of  $\text{HSO}_3^-$  and its derivatives in non-acidic ( $\text{pH} > 2.5$ ) waters. At  $T = 0^\circ\text{C}$ ,  $\text{HSO}_3^-$  and  $\text{SO}_3^{2-}$  concentrations are an order of magnitude higher than at  $T = 25^\circ\text{C}$ . Similarly, at  $T = 50^\circ\text{C}$ ,  $\text{HSO}_3^-$  and  $\text{SO}_3^{2-}$  concentrations are an order of magnitude lower than at  $T = 25^\circ\text{C}$ . Our overall conclusions are robust to these variations. However, this study does imply that significantly higher concentrations of  $\text{SO}_2$ -derived anions are available to prebiotic chemistry in cooler waters, and inversely that hotter waters would have access to lower levels of  $\text{SO}_2$ -derived anions.

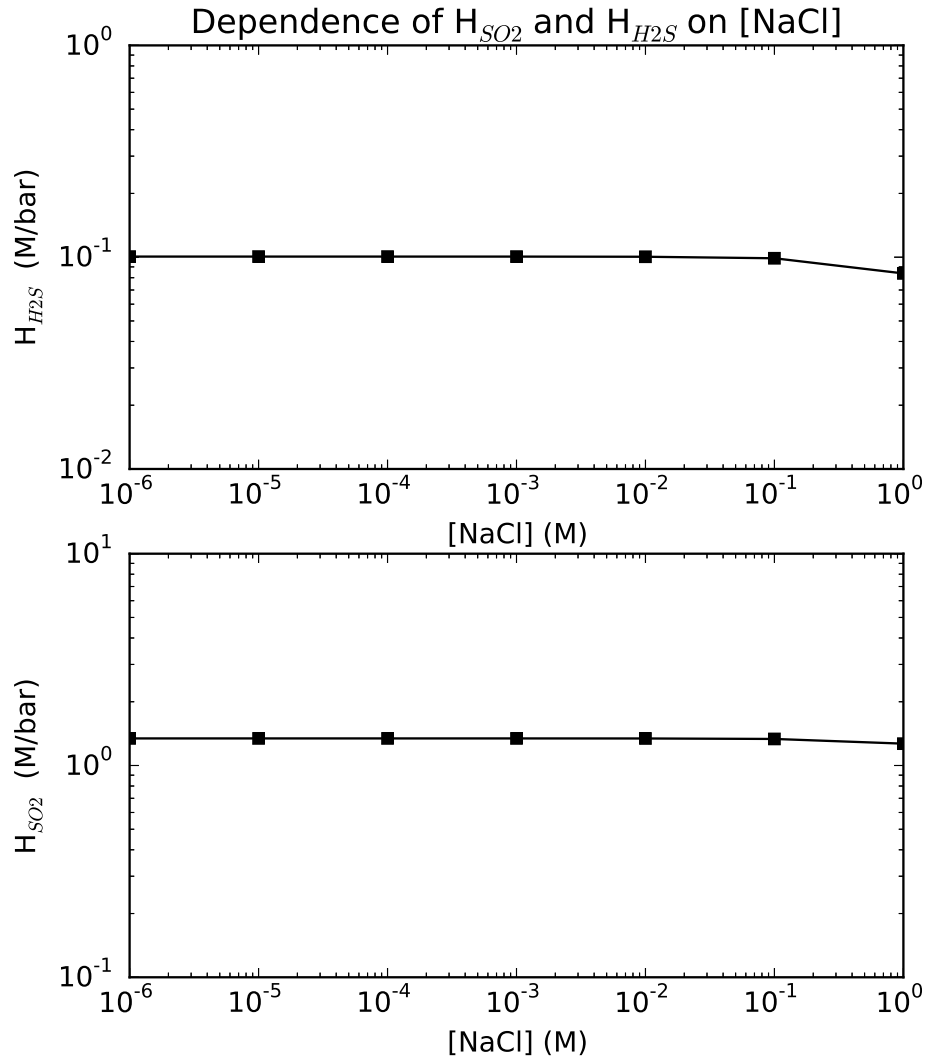


Fig. 6.— Dependence of Henry’s Law constants for  $H_2S$  and  $SO_2$  on  $[NaCl]$ , calculated using the formalism from Burkholder et al. (2015).  $H_{H_2S}$  and  $H_{SO_2}$  are insensitive to  $[NaCl]$  for  $[NaCl] < 1M$ .

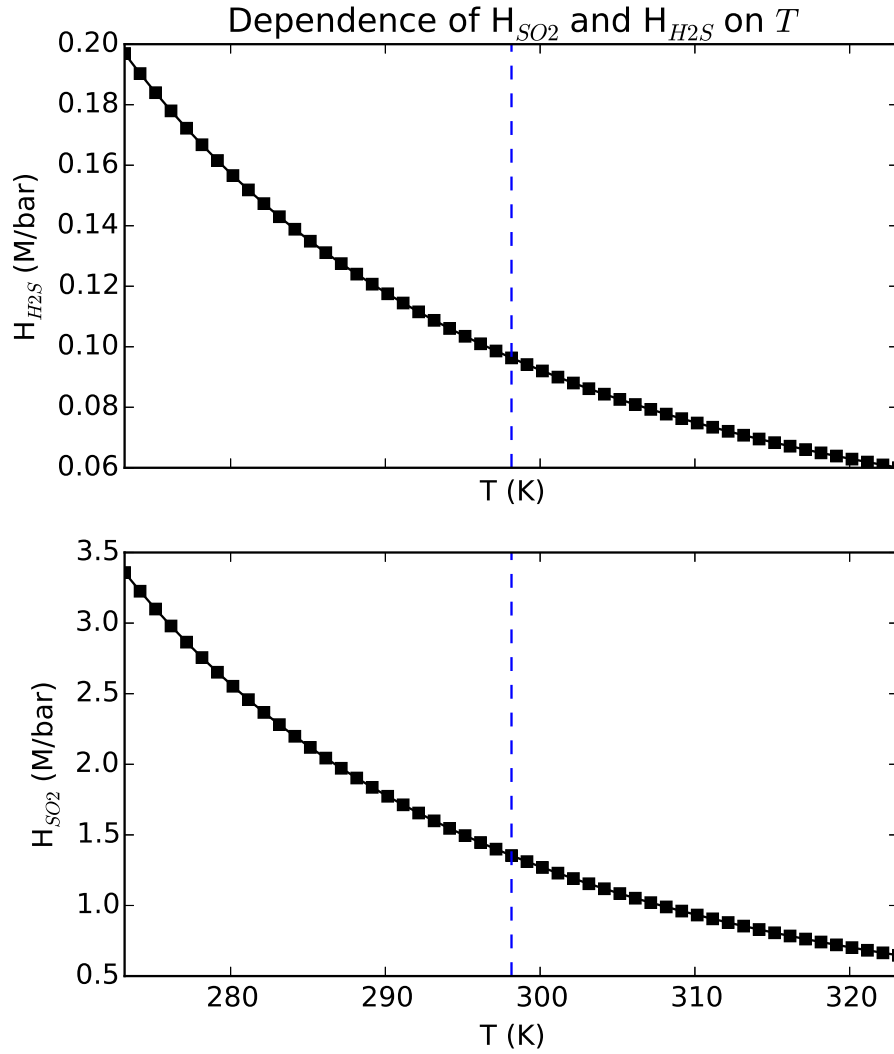


Fig. 7.— Temperature dependence of Henry’s Law constants for  $H_2S$  and  $SO_2$ , calculated using the formalism from Burkholder et al. (2015). Varying the temperature by 25K relative to the reference temperature of 298.15K (blue line) affects the value of  $H_{H_2S}$  and  $H_{SO_2}$  by less than a factor of 2.5.